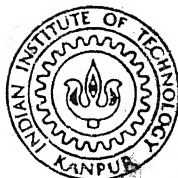


THEORETICAL STUDY OF THE REACTIONS INVOLVING DEUTERONS AND He^3

PRAVAT KUMAR PATTNAIK

TH
PHY/1969/D
P2786



DEPARTMENT OF PHYSICS
INDIAN INSTITUTE OF TECHNOLOGY
KANPUR

CENTRAL LIBRARY

ndian Institute of Technology

KANPUR

Thesis

Cl : No. 53.9:75.....

P278t

To my parents

Carnegie-Mellon University

Department of Physics
Schenley Park
Pittsburgh, Pennsylvania 15213
[412] 621-2600

March 6, 1969

This is to certify that the work presented in this
thesis has been carried out by Mr. Pravat Kumar Patnaik
under my supervision.

PHY-1969-D-PAT-THE

Bibhuti B. Deo

B. B. Deo
Associate Professor of Physics
Indian Institute of Technology
Kanpur, India

PROVOST'S OFFICE
This thesis has been approved
for the award of the Degree of
Doctor of Philosophy (Ph.D.)
in accordance with the
regulations of the Indian
Institute of Technology, Kanpur.
Deo
16/3/69

ACKNOWLEDGEMENTS

With great pleasure I thank Professor B.B. Deo for suggesting the problems and for his sincere guidance throughout the course of this work. He has introduced me to Physics and his long association as a teacher has been the most rewarding experience for me. I am thankful to Professor L. Wolfenstein for going through the manuscript and suggesting many improvements and to Professor R. Ramachandran for his constructive criticism. Thanks are also due to Prof. J. Mahanty for his active interest and sincere encouragements.

Most of the work reported in this thesis were presented in High Energy Physics group seminars at various stages of completion. I am thankful to all members of the group for hearing my talks patiently and offering their critical comments.

I am also thankful to Mr. H.N. Nigam for expertly typing, Mr. Lallu Singh for cyclostyling and Mr. H.K. Panda for his help in preparation of this thesis.

Last but not the least I am thankful to my wife Alaka without whose active cooperation and fine understanding this thesis could not have been completed. It is superfluous to thank my friends Krutibash and Surjyonanayan. They have been associated with me from early student days and have always stood side by side with me in agony as well as in ecstasy. Finally I thank all my friends who have made my stay at Kanpur pleasant and memorable.

CONTENTS

<u>Chapter</u>		<u>Page</u>
	LIST OF TABLES	
	LIST OF FIGURES	
	ABSTRACT	
I	INTRODUCTION	1
II	ONE PARTICLE EXCHANGE MODELS	6
	2.1 Perturbation Theory	6
	2.2 S-Matrix	8
	2.3 Alternatives to Perturbation Theory (Polology)	12
	2.4 One Pion Exchange Models	18
	(i) Phenomenological form factors	18
	(ii) Regge Poles	21
	(iii) Absorption Model	22
	2.5 One Nucleon Exchange Models	23
III	PROTON DEUTERON SCATTERING	26
	3.1 Impulse Approximation	26
	3.2 Method of Separable Potentials	29
	3.3 Nucleon Pole diagram	32
	3.4 The Vertex Functions and Form Factors	35
	3.5 Numerical Results and Discussions	41

<u>Chapter</u>		<u>Page</u>
IV	PION PRODUCTION IN PROTON DEUTERON COLLISION	44
	4.1 Matrix Elements	45
	4.2 He^3pd Vertex and Form Factors	48
	4.3 $\text{He}^3\text{He}^3\pi^0$ Coupling Constant	51
	4.4 Details of Trace Calculation	53
	4.5 Numerical Results	55
V	ROLE OF NUCLEON EXCHANGE IN GENERATING He^3 POLE	59
VI	ON THE EXISTENCE OF PEAKS IN THE CROSS SECTION OF THE REACTIONS, $\text{p}+\text{p} \rightarrow \text{d}+\pi^+$, $\text{k}+\text{d} \rightarrow \text{p}+\wedge$, $\text{p}+\text{d} \rightarrow \text{He}^3+\pi^0$	66
VII	CONCLUSION	72
	APPENDIX: MORE ABOUT npd VERTEX	74
	A1. Mathews-Deo Vertex	74
	A2. Generalised Vertex	75
	A3. Blankenbecler, Goldberger and Halpern Vertex	76
	A4. Form Factors and Deuteron Wave function	77
	REFERENCES	78

LIST OF TABLES

<u>Number</u>	<u>Caption</u>	<u>Page</u>
1	Differential cross section for $p+d \rightarrow He^3 + \pi^0$	57
2	Energy dependence of $\frac{d\sigma}{d\Omega} (10^{-30} \text{cm}^2)$ at centre of mass angle 180° for different values of r_c . $G_c = 2g_c$	58
3	Position of peaks for different final state particles in the reaction $p+d \rightarrow He^3 + X$	71

LIST OF FIGURES

<u>Number</u>	<u>Caption</u>	<u>Page</u>
1,2,3	Feynman diagrams for pion-nucleon scattering	10
4	Feynman diagram for nucleon-nucleon scattering with pion exchange	14
5	Pology in t-channel	14
6	Pion exchange diagram in the reaction $N + \pi \rightarrow N + \pi + \pi$	15
7	He^3 pole diagram in pd scattering	33
8	Nucleon pole diagram in pd scattering	34
9	npd vertex	36
10	Backward proton-deuteron scattering	42
11	Feynman diagram for single-proton exchange in $p+d \rightarrow \text{He}^3 + \pi^0$	46
12	Feynman diagram for $p+d \rightarrow \text{He}^3 + \pi^0$ in direct channel with He^3 pole	46
13	pd He^3 vertex	47
14	$\text{He}^3 \text{He}^3 \pi^0$ vertex	47
15	Differential cross section for the reaction $p+d \rightarrow \text{He}^3 + \pi^0$ at 0.6 Bev with $r_c = 0.05 F$	
16,17	Differential cross section for the reaction $p+d \rightarrow \text{He}^3 + \pi^0$ with $r_c = 0.052 F$	56
18	Box diagram for the reaction $p+p \rightarrow d + \pi^+$	68
19	Box diagram for the reaction $p+d \rightarrow \text{He}^3 + X$	68

ABSTRACT

The differential cross section for the reactions $p+d \rightarrow p+d$ and $p+d \rightarrow He^3 + \pi^0$ has been calculated taking Born diagrams alone. For this first reaction we evaluate backward scattering only where the nucleon exchange is most predominant. The He^3 pole contribution is found to be small. For the reaction $p+d \rightarrow He^3 + \pi^0$ we evaluate both nucleon and He^3 pole contributions. We set up npd , $PdHe^3$, $He^3He^3\pi^0$ vertices. The npd and $pdHe^3$ form factors which are related to the Fourier transform of deuteron and He^3 wave functions are obtained in closed form. The results are compared with the available experimental data and found to be in fair agreement. With the help of this pd amplitude we generate the He^3 pole by N/D method. As the binding energy of He^3 is small the residue at the pole can be obtained analytically. Finally we explore the possibility that the cross section of the reactions $p+p \rightarrow d + \pi^+$, $k+d \rightarrow p + \Delta$ and $p+d \rightarrow He^3 + \pi^0$ may have several peaks in them. We write down analytical expressions for the positions of the peaks. The experimental results obtained so far are consistent with our results.

CHAPTER I

INTRODUCTION

Recently there has been a great deal of interest regarding the elementarity of elementary particles. One group of people believe that there exists a set of particles which form a privileged class and all other mechanism can be understood through them. But, the other group believes that all nuclear particles can be dealt at the same level of elementarity. They give it a name, 'the nuclear democracy'.¹ But, most of the people still feel very much confused about this matter. Let us ask the question - what is an elementary particle? Is there any fundamental difference between a proton and a deuteron? An elementary particle is an elementary object which can not be further subdivided. It does not have any structure. Deuteron consists of two particles, neutron and proton. So it cannot be an elementary particle. The exponents of nuclear democracy do not agree to this assertion. They say that the difference between a proton and a deuteron is completely quantitative in nature and as such this difference is artificial. In an exact formulation of the bound state problem proton, for an example, can be considered as a bound state of (Λ, k) , in as much as the deuteron is a bound state of (n, p) .

This idea has been extended to what is now called Nuclear Democracy¹. In this rule of law all particles are based on the same footing. The forces that bind up two

particles are entirely due to particles being exchanged in the crossed channels. Then they are all connected through a set of bootstrap equations which in principle can be solved self consistently.

Although this idea is being pursued very seriously, one is not yet sure that the idea of nuclear democracy is correct. "It is too soon to tell with absolute certainty that there are no aristocrats among nuclear particles: theorists continue to investigate, for example, the possibility that certain spin one mesons may play a distinguishing role analogous to that of photon, with arbitrary masses and coupling constants. My stand point here, however, is that every nuclear particle should receive equal treatment under law."
(Chew).

In the absence of any definite criteria to distinguish elementary from composite particles or any definite assertion that they are the same we suggest a different approach. The theories and method that have been developed for so called elementary particles alone should be applied to the reactions involving composite particles like deuteron or He^3 . If they give good results we can say with some certainty that the composites are no different than elementary particles. To Weinberg,² however, there exist definite criteria which distinguishes between an elementary and a

where $Z = |\langle B_0 | B \rangle|^2$, the probability of finding a bare elementary particle in a stable dressed state. Z can be related to physically measurable quantities. He concludes that deuteron is a composite particle, not elementary.

At this point we do not enter into the controversy whether the Lagrangian theory is correct or not. It is quite plausible to think that there can be some approach within the frame work of Lagrangian method but different from perturbation theory. Even otherwise we know that there are many results which are easily obtained from the Lagrangian field theory, but can be otherwise obtained by a more cumbersome method. So instead of setting up a Lagrangian for the interacting system, we just start by writing down the vertex functions for composite particles. Then we calculate the differential scattering cross section from the pole diagrams and compare with the experiment where it is supposed to have best agreement. If we get good agreement we can say that they are as much elementary as any other particles.

In this thesis we have pursued this idea whole heartedly. To be specific, we have considered few reactions where He^3 and deuteron are involved and where nucleon exchange plays a dominant role. Although our results do not present themselves as very strong evidences in support of the nuclear democracy, they provide enough stimulation to keep our interests alive and take up further investigations. The lack

of good agreement may be due to our poor knowledge of deuteron and He^3 wave-functions.

In Chapter II we review the one-particle exchange processes. It is shown that perturbation theory fails for strong interaction processes, but the pole terms can still provide a good approximation in some specific cases. We also discuss form factors, Regge poles and absorption correction. The one nucleon exchange processes are slightly more difficult to understand than the one pion-exchange processes. At the end we survey a few papers on nucleon pole diagrams and give the idea of form factors.

In Chapter III the proton deuteron elastic scattering is discussed. Two methods are usually used for this study. They are the impulse approximation and the method of separable potentials⁸⁻¹⁰. These methods are briefly discussed. Then we go to the nucleon exchange diagrams. We obtain npd vertex, form factors and then proceed to calculate differential cross section in backward direction. This is compared with experiment and is found to have good agreement.

The Chapter IV deals with the reaction $p+d \rightarrow \text{He}^3 + \pi^0$. Here we construct pd He^3 and $\text{He}^3\pi$ vertices, calculate the cross section and compare with experiment.

In Chapter V we take a slightly different attitude. We generate the He^3 pole in pd amplitude by the exchange of a neutron in crossed channel. We obtain a pole with all the

quantum numbers of He^3 . But, the mass corresponding to the pole position is slightly more than He^3 . The position of the pole is dependent on the strength of the interaction. This tells that He^3 is a bound state of p and d. This, of course, we all know. But, this tells us one thing more that He^3 is a bound state of p and d exactly in the same way as N is a bound state of K and Λ .

In Chapter VI we investigate the existence of the peaks in the cross sections of the reactions, $p+d \rightarrow \text{He}^3 + X$, $p+p \rightarrow d+\pi^+$, $k+d \rightarrow p+\Lambda$. Some of the peaks have already been observed experimentally. We write down analytical expressions for the positions of the peaks without assuming the existence of two and three baryon resonances.

In appendix we discuss more about npd vertex following Mathews and Deo. We derive their results and utilise these results to obtain a general vertex which, in the neighbourhood of pole, goes to the results of Blankenbecler, Goldberger and Halpern.²³ At the end we show the explicit relation between the deuteron wave function and the npd vertex form factor.

CHAPTER IIOne Particle Exchange Models

2.1. Perturbation Theory:

In non-relativistic quantum mechanics the interaction between two particles can very well be described through a potential. A hamiltonian H can be defined which can be separated into two parts-kinetic energy and potential energy. In many cases the hamiltonian H can also be separated into two parts

$$H = H_0 + H_I \quad (1)$$

where H_0 is that part of hamiltonian for which the Schrödinger equation

$$H_0 \varphi = E \varphi_0 \quad (2)$$

can be solved exactly. With this we can make a perturbation calculation and obtain the solutions for perturbed eigenvalues and eigenfunctions. A necessary condition for perturbation theory to work is that H_I must be small compared to H_0 . In the relativistic theory we do not have any potential. But, we have an alternative approach which we call the local interactions between particles.

In a local field theory¹¹ every particle is represented by a field and a Lagrangian L can be constructed for each field such that the Euler-Langrange equations, we

get by the variation of L , are the corresponding field equations. The Lagrangian L can be separated into two parts L_0 and L_I where L_0 consists of lagrangians of free fields and L_I contains the interaction between the particles. To write down L_I explicitly we take the following considerations into account.

1. L_I must be a Lorentz scalar.
2. The field equations must be linear in field operators.
3. There should not be any derivative coupling.

When we apply all these three restrictions we find that we have a very limited choice to make. For a spinor ψ interacting with a vector field A_μ , we get

$$L_I = g_e (\bar{\psi} \gamma^\mu \psi) A_\mu \quad (3)$$

and for a spinor field interacting with a pseudoscalar field

$$L_I = g_s (\bar{\psi} \gamma_5 \psi) \phi \quad (4)$$

where g_e and g_s are the coupling constants measuring strength of interaction. If A_μ stands for electromagnetic field we have

$$g_e^2 / 4\pi = 1/137$$

and if ϕ stands for pion field

$$g_s^2 / 4\pi = 15.$$

Once we know L_I we can know H_I very easily. For non-derivative couplings this is just the negative of L_I .

2.2. S-Matrix

From the interaction hamiltonian H_I we can construct the S-matrix which in turn is related to the scattering amplitude. A perturbation theory can best be worked in interaction picture. The S-matrix is defined as

$$S = \lim_{t_2 \rightarrow \infty} \lim_{t_1 \rightarrow \infty} \langle \varphi_b | U(t_2, t_1) | \varphi_a \rangle \quad (5)$$

where $U(t_2, t_1)$ is the time displacement matrix given by the equation

$$i \partial_t U(t, t_0) = H_I(t) U(t, t_0) \quad (6)$$

or equivalently by the integral equation

$$U(t_1, t_0) = 1 - \frac{i}{\hbar} \int_{t_0}^{t_1} H_I(t) U(t, t_0) dt \quad (7)$$

By the process of successive iteration we will get the Newmann-Liouville expansion of the integral (7) as

$$\begin{aligned} U(t, t_0) &= 1 + (-i/\hbar) \int_{t_0}^t dt_1 H_I(t_1) \\ &+ (-i/\hbar)^2 \int_{t_0}^t dt_1 \int_{t_0}^{t_1} dt_2 H_I(t_1) H_I(t_2) \\ &+ \dots \end{aligned} \quad (8)$$

From this we obtain the S-matrix after making some manipulations to take the limit. We get

$$S = \sum_{n=0}^{\infty} (-i/\hbar)^n (1/n!) \int_{-\infty}^{+\infty} d^4 x_1 \dots \int_{-\infty}^{+\infty} d^4 x_n P(H_I(x_1) H_I(x_2) \dots H_I(x_n)) \quad (9)$$

P is the Dyson's chronological operator. For further developments on this we have to assume a specific type of interaction. Then the S-matrix is given by the following series.

$$\begin{aligned}
 S = 1 &+ (-ig/\hbar) \int d^4x_1 \bar{\psi}(x_1) \gamma_5 \psi(x_1) \phi(x_1) \\
 &+ (-ig/\hbar)^2 \int d^4x_1 \int d^4x_2 T(\bar{\psi}(x_1) \gamma_5 \psi(x_1) \phi(x_1) \\
 &\quad \bar{\psi}(x_2) \gamma_5 \psi(x_2) \phi(x_2)) \\
 &+ \dots \dots \dots \quad (10)
 \end{aligned}$$

From the above expansion it is possible for us to extract the matrix elements for any process involving nucleons, antinucleons and pions. All these processes can be symbolically represented by a set of diagrams usually called Feynman diagrams. There are specific rules (Feynman rules) to calculate matrix elements from these diagrams. The matrix elements can be written down either in p-representations or in x-representations. For most of the time we will work in p-representation.

To discuss some more specific properties of S-matrix it will be useful to consider a specific physical situation. We will consider the pion-nucleon scattering. The first contribution to pion nucleon scattering comes from the third term. There are two diagrams and the matrix elements are given by (Figs. 1 and 2)

$$M_1 = g^2 \bar{u}(p') \gamma_5 \frac{1}{\gamma \cdot (p-k') - m} \gamma_5 u(p)$$

$$M_2 = g^2 \bar{u}(p') \gamma_5 \frac{1}{\gamma \cdot (p+k) - m} \gamma_5 u(p) \quad (11)$$

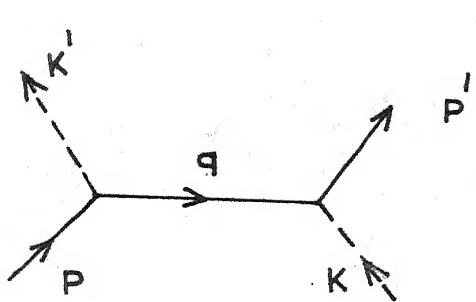


FIG. 1

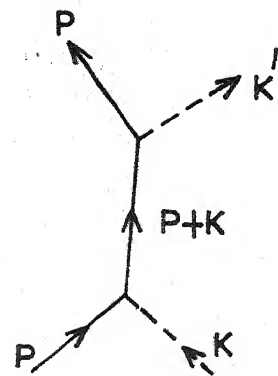


FIG. 2

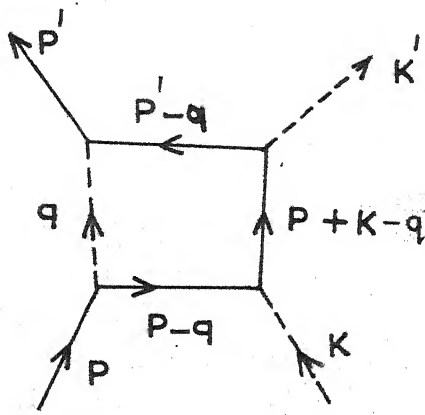


FIG. 3

FEYNMAN DIAGRAMS FOR PION-NUCLEON SCATTERING

There can be contributions from higher order of terms also. One such example is given by the figure 3 where we get

$$M_3 = g^4 / (2\pi)^4 \int d^4 q \frac{1}{q^2 - \mu^2} \cdot \bar{u}(p') \gamma_5 \frac{1}{\gamma \cdot (p' - q) - m} \gamma_5$$

$$\frac{1}{\gamma \cdot (p + k - q) - m} \gamma_5 \frac{1}{\gamma \cdot (p - q) - m} \gamma_5 u(p) \quad (12)$$

Similarly we can have contributions from higher order diagrams. Now the question arises - what should we do to calculate the transition amplitude? Should we sum up all possible diagrams upto infiniteth order or should we stop at some suitable point? This question is linked with the convergence of the perturbation series. The first requirement is that the series should be convergent. Then there is another question - even if the series is convergent can all possible types of diagrams be summed? This is possible for some particular type of diagrams like ladder diagrams. But, all diagrams cannot be summed up. So the only alternative possibility for a reliable theory is that g should be very small such that the series is rapidly convergent and the first few terms of the expansion can give a fair estimate of the process involved. This is true in quantum electrodynamics where $g_e^2/4\pi = 1/137$. The second order term is sufficient to give very accurate results. But, this is not true for pion nucleon scattering where $g_S^2/4\pi = 15$. The series is not convergent. So we must find a way out of this difficulty.

In the next section we will try to obtain an

alternative to perturbation theory. Historically there have been approaches like Tamm-Dancoff methods¹², Chew-Low theory¹³ or dispersion-relations¹⁴ etc. But, our main aim will be to extract as much information as possible from the figures 1 and 2 and to see in what circumstances we can do so. The matrix element M_1 can also be written as

$$M_1 = g^2 \bar{u}(p') \frac{y(p-k)-m}{(p-k)^2-m^2} u(p) \quad (13)$$

We can see that there is a pole at $(p-k)^2 = m^2$. This pole is away from the physical region. But, in some cases this pole is very close to the physical region and for that region the contribution from the pole diagram (1 and 2) will be significant.

2.3. Alternatives to Perturbation Theory (Polology)

We have come to the conclusion that the perturbation theory can not be applied to strong interaction physics. There have been attempts to formulate theories that can replace perturbation theory, but not all of them have survived. Of all the theories the dispersion relations have been most useful in getting some results in strong interaction physics. Here we will not deal with dispersion relations, but will use some of the results obtained by dispersion relations.

It is well known¹⁵ that the scattering amplitude can be written down in terms of a set of poles and cuts in terms of s , t and u . Our present aim is to find out the

situation where these poles are most predominant. This is called polology. For example consider the scattering of two spinless nucleons through the exchange of a scalar meson. Symbolically this can be represented by the figure 4. The matrix element is given by

$$M = \frac{g^2}{t - \mu^2} \quad (14)$$

$$\text{where } t = (p_1 - p_1')^2 = -2q^2(1 - \cos \theta) \quad (15)$$

In the neighbourhood of $t = \mu^2$ M will be most predominant and can provide a reasonable estimate of the actual matrix element. At the pole

$$-2q^2(1 - \cos \theta) = \mu^2$$

$$\text{giving } \cos \theta = 1 + \mu^2 / 2q^2 \quad (16)$$

The equation(16) tells that the pole is completely outside the physical region (see figure 5). But for very high energy $q^2 \rightarrow \infty$ and $\cos \theta \rightarrow 1$. This suggests that for very high energy the pole term in t-channel can give good estimate of the cross-section in forward direction ($\cos \theta = +1$). Actually this procedure has been used to calculate the coupling constant by extrapolating the experimental data to pole position ($\cos \theta = 1 + \mu^2 / 2q^2$). Another example of polology is the single pion production in pion-nucleon interaction. The matrix element (see fig. 6) is given by

$$M = \frac{g}{t - \mu^2} \bar{u}(p') \gamma_5 u(p) M_0 (q_1 + q_2 \rightarrow q_3 + q_4) \quad (17)$$

If we know the differential cross section for the process at

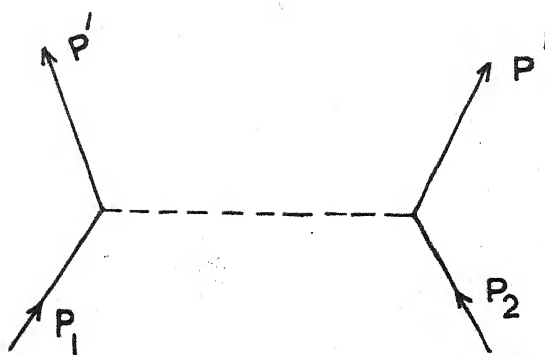


FIG. 4

FEYNMAN DIAGRAM FOR
NUCLEON-NUCLEON SCATTERING WITH PION EXCHANGE.

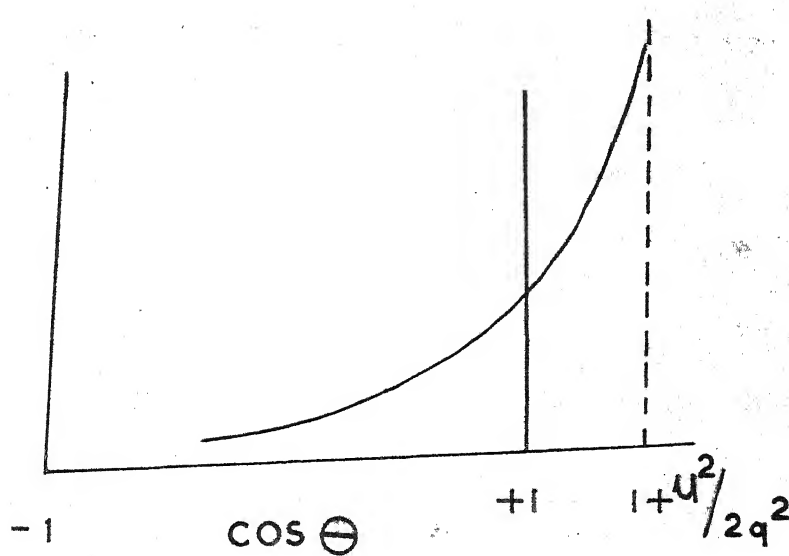


FIG. 5

POLOLOGY IN T-CHANNEL

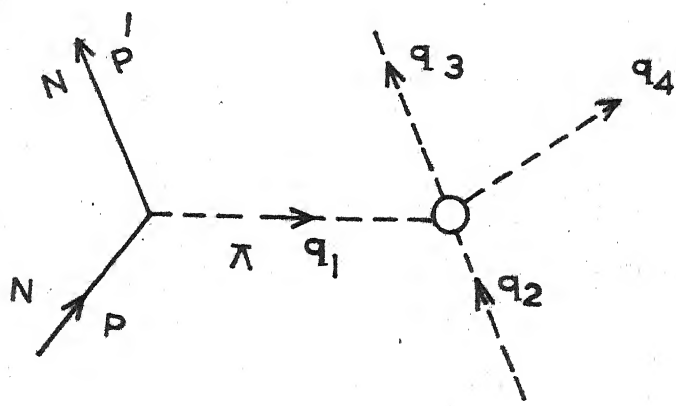


Fig. 6

PION EXCHANGE DIAGRAM IN THE REACTION $N + \Lambda \rightarrow N + \Lambda + \Lambda$

very high energy and close to the pole we can extrapolate the data to the pole and obtain the value of differential cross section for pion pion scattering. Conversely, if we know the pion pion scattering cross section we can evaluate the cross section (17) very easily near the pole position.

Thus, we come to the conclusion that at very high energy the differential cross section in forward direction ($\cos \theta = +1$) can reasonably be represented by t-channel pole diagrams (i.e. the poles originated due to meson exchanges). Then the natural inclination is to ask - what happens when a baryon is exchanged instead of a meson? To answer this question we will deal with pion nucleon scattering (fig. 1). The matrix element is

$$M = g^2 \bar{u}(p') \gamma_5 \frac{\gamma \cdot p + m}{u - m^2} \gamma_5 u(p) \quad (18)$$

$$u = (p - k')^2 = m^2 + \mu^2 - 2[E_p w + q^2 \cos \theta]$$

$$\text{For very high energy } E_p = (q^2 + m^2)^{\frac{1}{2}} = q[1 + m^2/2q^2]$$

$$w = q[1 + \mu^2/2q^2]$$

$$\text{and } u = -2q^2(1 + \cos \theta)$$

So, at the pole, we obtain

$$\cos \theta = -1 - m^2/2q^2 \quad (19)$$

The expression looks quite familiar. For $q \rightarrow \infty$ we again get the pole dominance and rest of the things follow as in the case of one meson exchange.

What we have done above is a phenomenological

analysis. To give it a more fashionable look we consider the Mandelstam representation.¹⁵ If we assume that this representation is correct, then, in certain cases we can justify the pole dominance of forward and backward amplitude. For spinless nucleon nucleon scattering, assuming no subtraction, the Mandelstam representation takes the form

$$\begin{aligned}
 T(s, t, u) = & \frac{g^2}{t - \mu^2} + \frac{g^2}{u - \mu^2} + \frac{1}{\pi} \int \frac{dt' f_1(t')}{t' - t} + \frac{1}{\pi} \int \frac{ds' f_2(s')}{s' - s} \\
 & + \frac{1}{\pi} \int \frac{f_3(u') du'}{u' - u} + \frac{1}{\pi^2} \int \frac{f_1(s', t') ds' dt'}{(s' - s)(t' - t)} \\
 & + \frac{1}{\pi^2} \int \frac{f_2(s', u') ds' du'}{(s - s)(u' - u)} + \frac{1}{\pi^2} \int \frac{f_3(u, t) du' dt'}{(u' - u)(t' - t)} \quad (20)
 \end{aligned}$$

$$\text{with } s + t + u = 4m^2 \quad (21)$$

For high energy forward scattering, t is fixed, $s \rightarrow \infty$ and because of relation (21) $u \rightarrow \infty$. Then equation (20) becomes

$$T(t) = \frac{g^2}{t - \mu^2} + \frac{1}{\pi} \int \frac{f_1(t') dt'}{t' - t} = \frac{g^2(t)}{t - \mu^2} \quad (22)$$

where $g^2(t)$ is smooth function with $g^2(\mu^2) = g^2$. This final result consists of contributions from single intermediate pion lines. A similar formula can also be obtained for nucleon poles. Thus we see that the nucleon pole contributes to the backward direction exactly in the same way meson poles contribute to forward scattering. But, there is a difference. For meson pole $\cos\theta = 1 + \mu^2/2q^2$ and for nucleon pole $\cos\theta = -1 - m^2/2q^2$. So for $q^2 \rightarrow \infty$ the meson pole moves faster towards the physical region than the nucleon pole. As

a result of this the treatment of nucleon pole needs more care than the treatment of meson poles.

2.4. One Pion Exchange Models¹⁶

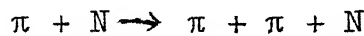
As a single particle exchange model offers a straight forward method of calculation it is easy to carryout the calculation far inside the physical region away from the single particle exchange pole and compare the results with the experiment. It is not surprising that such procedure fails in reproducing the exact experimental result. The reason is that far inside the physical region we can not treat the exchanged particle as a quasi-real particle. An off-the-mass-shell correction has to be made and many particle exchange graphs should also be considered to give reliable result. Now a days three types of off-shell corrections are usually used. They are

- (i) Use of phenomenological form factors
- (ii) Regge Pole models
- (iii) Absorption corrections.

Here we will describe briefly each of the three approaches.

(i) Phenomenological form factors:

We again turn to the reaction (fig. 6)



In addition to formation of nuclear isobars in the scattering channel which contributes calculable amounts to the scattering

amplitude over known energy and momentum range there are poles in matrix elements coming from the peripheral exchange of particles. The lightest particle exchanged in this case is a pi meson and has a pole very close to the physical region which is expected to influence the reaction.

Direct experimental evidence for the assumption is provided by the marked forward peaking in the cross section. According to Feynman rules the amplitude for such a process can be written as

$$T = V_A V_B / (t - \mu^2) \quad (23)$$

where V_A and V_B are vertex functions. These vertex functions contain all the corrections to the vertices due to off-shell nature of exchanged particle, but do not contain initial or final state interactions. This πNN vertex can be written as

$$V_{\pi NN} = g \bar{u}(p_2) \gamma_5 u(p_1) F(t) \quad (24)$$

where \bar{u} and u are the final and initial Dirac spinors for the nucleons. g is the pion nucleon coupling constant with $g^2/4\pi = 15$. $F(t)$ is the form factor with $F(\mu^2) = 1$ and obeys a dispersion relation (for the $NN\pi$ vertex),

$$F(t) = 1 + \frac{t-\mu^2}{\pi} \int \frac{\sigma(t') dt'}{9\mu^2 (t - \mu^2)(t - t')} \quad (25)$$

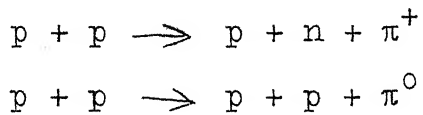
The weight function in the spectral integral has a threshold at $t = 9\mu^2$ corresponding to the square of the least massive state that can be coupled to pion.

There are analogous form factors corresponding to $\pi\pi$ vertex which depend on the distance of the exchanged pion from the mass shell. These form factors depend only on momentum transfer. In actual calculation it is very difficult to calculate the form factors. So in most cases we have to use phenomenological form factors that give good fits. They are supposed to be an one effective pole approximation to the contributions from the cuts.

This form factor approach has been applied extensibly by Ferrari and Selleri. An excellent review upto 1962 is also given by these two authors.¹⁷ A more recent discussion is also given by Selleri.^{17a} Now coming back to equation 23 we note that we have written down the product of two form factors. In actual practice these form factor are phenomenologically fitted. Ferrari and Selleri used a particular type of form factor i.e.

$$G(t) = A - \frac{B\mu^2}{t - c\mu^2} \quad (26)$$

where A, B and C are obtained from the best fit with experiment. From the analysis of two processes



Ferrari and Selleri found $A = 0.28$, $B = 3.42$, $C = 5.75$ which gave good fits upto 1 Bev. A significant aspect of this analysis was that these values could also be used for pion exchanges in other reactions like $\pi + N \rightarrow p + N$ or $\pi + N \rightarrow \pi + N$.

In short, once the form factor was known from one reaction, it could be used for a set of reactions.

The form factor approach has draw back also. Being purely a phenomenological model there is no direct link between this and the physical situations. For example, a pole in the form factor is customarily associated with a resonance. Here in this particular case the resonance mass (2.4μ) given by Ferrari and Selleri is just too small to correspond to any known particle or resonance. Secondly the form factor approach fails for the energy larger than 1 or 2 Bev.

(ii) Regge Poles:

Several authors¹⁸⁻²⁰ have treated the exchanged particles as Regge poles. This has the required effect of reducing the high energy cross section, but introduces too many parameters. Especially for elastic scattering the number of exchanged particles is too large. Consequently the number of unknown parameters are very large. The usefulness of the model can be tested only in the case when the number of particle-exchanges are small (preferably one or two). In many cases a single exchange has given very good fit to the cross section. This model has been useful in predicting several high energy results otherwise impossible to obtain. Another attractive feature of the model is that the usual pole term is replaced by a term which is the function of Regge trajectory. The introduction of this trajectory takes care of a number particles lying over that trajectory. On

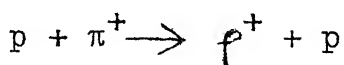
the dark side, as we have mentioned, the number of parameters are large and there exists a lower limit for each reaction bellow which this model can not be applied fruitfully.

In pd scattering nucleon exchange Born-diagram gives too low a cross section at backward angles at high energy due to the rapid decrease of the deuteron form factor. Exchange of a baryon resonance of requisite quantum number may compensate for this rapid decrease. Kisslinger and Kerman³² report that this may indeed explain the backward cross section. It would suggest that at high energy baryon exchange be reggized.

(iii) Absorption Model²¹:

The main idea behind the absorption correction is very simple. Due to the influence of competing channels the inelastic scattering amplitude gets modified (rather damped). Theoretically the most complete theory was given by Baker and Blankenbekler.²² Unfortunately their theory does not give correct t-dependence. All other theories deal with parametrization with a view to give the immediate result.

Consider the reaction



For this reaction absorption correction is obtained in the following manner. First obtain the helicity amplitudes and then make a partial wave decomposition. If $A(W)$ is the helicity amplitude we have

$$A_{\lambda_1 \lambda_2 \lambda_3 \lambda_4}^{(W)} = \sum_J \frac{(2J+1)}{2} \langle \lambda_3 \lambda_4 | a^J | \lambda_1 \lambda_2 \rangle d_{\mu}^J(\theta)$$

$$\text{with } \lambda = \lambda_1 - \lambda_2 ; \mu = \lambda_3 - \lambda_4$$

Now due to absorption in initial and final states the amplitude

$$\langle \lambda_3 \lambda_4 | a^J | \lambda_1 \lambda_2 \rangle$$

gets modified to

$$e^{i\delta_f^J(W)} \langle \lambda_3 \lambda_4 | a^J | \lambda_1 \lambda_2 \rangle e^{i\delta_i^J(W)}$$

where δ_i and δ_f are the phase shifts in initial and final state channels. Next these modified amplitudes summed up to give the modified scattering amplitudes. In practice the summation is replaced by an integration. But, that is not all. The presence of $d_{\mu}^J(\theta)$ poses a problem for integration. So usually the calculation is done for very small value of θ where $d_{\mu}^J(\theta)$ can be approximated by a Bessel function.

For pion exchange processes the absorption model has been quite successful. But, it fails for ρ exchange. For example consider the reaction

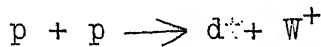


This reaction can not be fitted by one pion exchange. If we take the ρ exchange we obtain a theoretical cross section which is too large compared to experimental value at high momentum transfer.

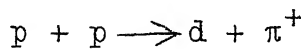
2.5. One Nucleon Exchange Models

Calculations based on one nucleon exchanged models are

very small. Few years back Blankenbecler, Goldberger and Halpern²³ studied the neutron deuteron scattering from dispersion theory. They obtained the contributions from nucleon pole as well as triton pole. From that time till now their results about npd and ndt vertices are being used by all authors who deal with these topics. Then there was a calculation by Bernstein²⁴ on vector boson production. He studied the reaction



with the help of one neutron exchange mechanism. Later Nearing repeated the same calculation. Nearing²⁵ made the calculation on the pole without the form factor, without taking deuteron structure into account. As the existence of vector meson is still a doubtful proposition this could not be compared with experiment. It was Deo and Mathews²⁶ who pointed out that the estimates given by Nearing is much larger than what it should actually be because he has left the form factors. These form factors are proportional to the Fourier transforms of s and d state deuteron wave functions. Then the reaction

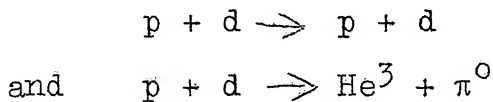


was studied by Mathews and Deo,²⁶ Deo and Patnaik²⁷ and Heinz et al.²⁸ The approaches in all these papers remain almost same. They all calculate the Born matrix elements and multiply the matrix element with suitable form factors.

In all the above calculations some of the prominent features of the experiment are reproduced, but many more questions remain unanswered. For the reaction $p + p \rightarrow d + \pi^+$ there is also a meson exchange diagram which was discussed by Yao²⁹. Yao believes that neutron exchange can not produce all the desirable features. However, Heinz²⁸ has compared one pion exchange and one neutron exchange model predictions and has shown if one has to choose one between the two models, it is neutron exchange model which gets the preference. However, Brown³⁰ shows that neither of the model can as such explain fully the experiment in the interval 3-13 Bev/c proton momentum.

There is still another reaction where nucleon pole contribution has been evaluated. This is the photo disinteg- ration of deuteron. Gourdin³¹ et al. have studied this process using two pole and four pole fits to the form factors.

In this thesis we will calculate the differential cross section for the two processes



with nucleon pole and He^3 pole contributions. The He^3 pole gives very small contribution to the first reaction. So the first reaction will be calculated with nucleon exchange alone. Then we will investigate the role of neutron exchange in generating He^3 pole in pd amplitude. This we will do by the help of N/D method.

CHAPTER III

PROTON DEUTERON SCATTERING

Deuteron has two properties which attract the attention of theoreticians as well as experimentalists. It is the simplest bound state of two strongly interacting particles and its binding energy is very small. As its binding energy is small we can use impulse approximation. As it is a simple two body bound state it can be used as a target particle to explore the nature of three body forces. Here we will briefly describe two methods-impulse approximation⁵⁻⁷ and method of separable potentials⁸⁻¹⁰ which have been extensively used to study deuteron scattering.

3.1. Impulse Approximation:

Neutron, as a target for bombarding particles, is difficult to get making it almost impossible to get a measurement of direct neutron cross section. In most of the cases it is being deduced from the proton-deuteron scattering. (From this point of view proton deuteron scattering was treated to be one of the most useful methods of investigation). As neutron and proton are very loosely bound inside deuteron it was thought that the proton deuteron scattering cross section can be expressed as the sum of np and pp cross section especially when the de Broglie wavelength of the bombarding particle is small compared to the average distance

of neutron and proton inside deuteron. It was Glauber who first analysed the proton deuteron scattering data and pointed out that the sum of the pp and pn cross section is somewhat larger than the pd scattering cross section. Glauber's analysis can be written down in the following form:

$$\sigma_{(pd)} = \sigma_{(pp)} + \sigma_{(pn)} - S \quad (1)$$

where S is an additional term usually called the shadow term or eclipse term.

$$S = \sigma_{(pn)} \sigma_{(pp)} \frac{\langle r^{-2} \rangle}{4\pi} \quad (2)$$

$\langle r^{-2} \rangle$ is the average value of the inverse square separation between proton and neutron inside deuteron. Here we give a simplified version of Glauber's analysis. For simplicity we will assume that all the particles are scalars. If we assume that the nucleons have a common mass M and deuteron mass is M_D , the binding energy of deuteron is $2M - M_D$. Let $\Psi(\mathbf{r})$ be the normalised deuteron wavefunction where \mathbf{r} is the separation between neutron and proton. The momentum space wavefunction is given by

$$\Psi(\mathbf{p}) = \frac{1}{(2\pi)^{3/2}} \int d^3\mathbf{r} \Psi(\mathbf{r}) e^{i \vec{p} \cdot \vec{r}} \quad (3)$$

Then we define the deuteron form factor $G(p^2)$ by

$$\begin{aligned} G(p^2) &= \int d^3\mathbf{r} |\Psi(\mathbf{r})|^2 e^{i \vec{p} \cdot \vec{r}} \\ &= \int d^3\mathbf{q} \Psi(\mathbf{p} - \mathbf{q}) \Psi(\mathbf{q}) \end{aligned} \quad (4)$$

such that $G(0) = 1$.

If we normalise scattering amplitude such that

$$\frac{d\sigma}{dt} = |F(s, t)|^2$$

The optical theorem becomes

$$\sigma(s) = 4\pi \operatorname{Im} F(s, 0)$$

In the rest system of deuteron, both n, p as well as d are at rest. So at high energy limit $S_{pp} = S_{pn} = 1/2 S_{pd}$ where S_{pp} , S_{pn} and S_{pd} are centre of mass energy squared. Then the result of Glauber's analysis is

$$\begin{aligned} F_{pd}(s, t) = & G(-t/4) [F_{pp}(s_{pp}, t) + F_{pn}(s_{pn}, t)] \\ & - \frac{i}{(2\pi)^{3/2}} d^2 p G(p^2) F_{pp} [s_{pp}, -(\frac{\vec{q}}{2} + \vec{p})^2] \\ & \times F_{pn} [s_{pn}, -(\frac{\vec{q}}{2} - \vec{p})^2] \end{aligned} \quad (5)$$

where $q^2 = -t$ and the angle of two dimensional vector q is the azimuth of the scattering. The integration $d^2 p$ is over the plane perpendicular to incident direction. If we use the optical theorem we obtain

$$\begin{aligned} \sigma_{pd} = & \sigma_{pn} + \sigma_{pp} - \frac{2}{\pi} R_e G(p^2) F_{pp}(s, -p^2) \\ & \times F_{pn}(s, -p^2) d^2 p \end{aligned} \quad (6)$$

where we have used the result $G(0) = 1$ and made the approximation that F_{pp} and F_{pn} are purely imaginary and the amplitudes are not rapidly varying over the range of integration. Then we bring these quantities outside the integration sign and write

$$\sigma_{pd} = \sigma_{pp} + \sigma_{pn} - \frac{1}{8\pi^2} \sigma_{pn} \sigma_{pp} \int G(p^2) d^2 p \quad (7)$$

$$= \sigma_{pp} + \sigma_{pn} - \frac{1}{4\pi} \sigma_{pn} \sigma_{pp} \langle r^{-2} \rangle \quad (8)$$

where $\langle r^{-2} \rangle = \frac{1}{2\pi} \int G(p^2) d^2 p$ is the average inverse square distance between the nucleons inside deuteron.

This formula was re-examined by Udgaonkar and Gell-mann⁶ from Regge pole theory. Their result for the eclipse term was given by the expression

$$\begin{aligned} \text{Im } F_{pd}^e(s, t) = & - \frac{\sigma_p \sigma_n}{8\pi^2} \text{Re} \int d^2 p G(p^2) B \left(-(\vec{p} - \vec{q}/2)^2 \right. \\ & \times B \left(-(\vec{p} + \vec{q}/2)^2 \right) \left(\frac{s}{s_0} \right)^\alpha \left[-(\frac{\vec{q}}{2} - \vec{p})^2 \right] \left[-(\frac{\vec{q}}{2} + \vec{p})^2 \right] - 2 \end{aligned} \quad (9)$$

This formula can be obtained by writing

$$F(s, t) = \frac{i}{4\sqrt{\pi}} \sigma B(t) \left(\frac{s}{s_0} \right) ^{\alpha(t)-1} \quad (10)$$

where $B(0) = 1$. This formula has been further modified by Abers et al.⁷ who found that at high energy the contribution of shadow term is less than that given by Glauber term. They also pointed out that at very high energy the shadow effect may slightly increase with energy. But, it must be remembered that till now all the analysis are done by the theory due to Glauber.⁵

3.2. Method Of Separable Potentials:

Next to the impulse approximation the method of

separable potentials has become one of the most useful tool in dealing with p-d scattering. The method is essentially non-covariant, but it gives very good fits particularly at low energy. The motivation for the calculations using separable methods comes from the following lines. A non-local separable potential yields a two body T-matrix which is also separable in off-shell variables. Then the Fadeev equations³³ with separable two body matrices become Fredholm equations in one variable only.

Many recent treatments aspire for the relativistic generalisation of three particle system. For this purpose Fadeev equation is favoured because this is expressed in terms of amplitudes rather than the potentials. It was pointed out by Gillepsie³⁴ that the potential method is no way less fundamental. More ever, the powerful techniques now available suggests that clearer insight and greater consistency is achieved by concentrating on the interaction operator (i.e. the potential) in any practical calculation.

The source of interaction term can be chosen from a particular model or can be constructed from experimental data. These methods were extensively studied by Mitra and his co-workers. Mitra constructed a potential of the type

$$v_1(p, p') = \lambda g_1(p) g_1(p') \quad (10a)$$

As we are not directly interested in these methods and our interest in the subject is only marginal we stop our discussion

here. A complete reference on the subject is given by Gilepsie³⁴ and Alessandrini³⁵ et al. To exhibit the power of separable methods we just solve one integral equation trivially which could have been much more difficult to do. Consider an integral equation for scattering amplitude M .

$$M_1(p, p_1) = V_1(p, p_1) + \int f(k) V_1(p, k) M_1(k, p_1) dk \quad (11)$$

where $V_1(p, p_1)$ is a Mitra type separable potential (equation 10) and $f(k)$ is a non-singular function. Then

$$M_1(p, p_1) = V_1(p, p_1) + g_1(p) \int dk f(k) g_1(k) M_1(k, p_1) dk \quad (12)$$

Multiply both sides by $f(p) g_1(p)$ and integrate with respect to p . Then we obtain

$$A(p_1) = \int dp f(p) g_1(p) V_1(p, p_1) + A(p_1) \int dp f(p) g_1^2(p) \quad (13)$$

where

$$A(p_1) = \int dk f(k) g_1(k) M_1(k, p_1) \quad (14)$$

The solution to equation B is given by

$$A(q) = \frac{\int dp f(p) g_1(p) V_1(pq)}{1 - \int dp f(p) g_1^2(p)} \quad (15)$$

$$\text{or } M_1(pq) = \frac{V_1(pq)}{1 - \int dp f(p) g_1^2(p)} \quad (16)$$

3.3. Nucleon Pole Diagrams:

When we look to the experimental results of proton deuteron cross section we observe two prominent peaks - one in forward direction and one in backward direction. As we have explained it earlier the forward peak is due to exchanges in the t-channel which can be iso-singlet mesons. The number of such particles are rather large and their interactions with deuteron is unknown. So any attempt to calculate forward scattering amplitude will involve several unknown parameters. On the otherhand the backward peak is essentially due to the nucleon exchange. The nucleon exchange diagram involves $NN\pi$ vertex which is known and npd vertex which can be obtained in a closed form. A form factor for this vertex can also be obtained with the help of non-relativistic Schroedinger theory of deuteron. This form factor takes into account the off-shell nature of exchanged nucleon and also the structure of deuteron. The matrix element for nucleon exchange diagram (fig. 7) can be written as

$$M = \bar{u}(p') S(d) \frac{\gamma_{n+m}}{n^2 - m^2} \bar{S}(d') u(p) \quad (17)$$

where $S(d)$ stands for npd vertex. There is also another diagram (fig. 8) which contributes to the scattering cross section. This is the He^3 -pole diagram. The contribution from this diagram is very less compared to the contribution from (fig. 7). This can be observed even without detailed calculation. We observe that the pole terms are the most

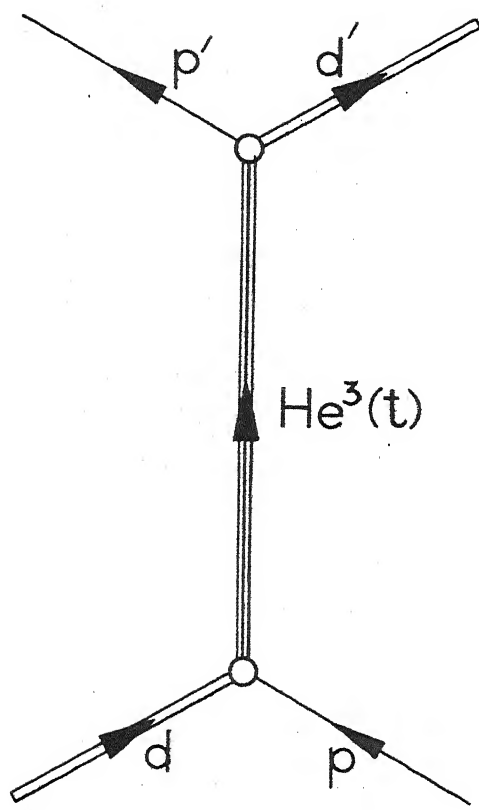


FIG. 7

He^3 pole diagram in scattering of pd

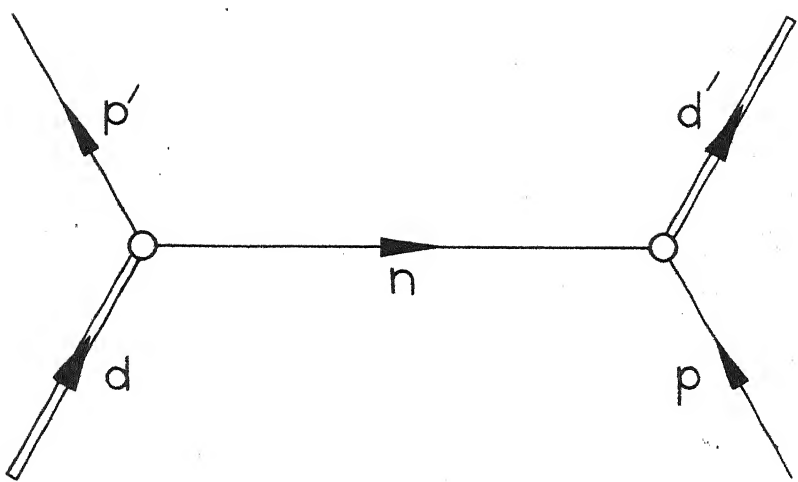


FIG.8

Nucleon pole diagram in $p d$ scattering

rapidly varying terms. At zero energy

$$n^2 = (M_d - m)^2$$

$$\text{So } n^2 - m^2 = (M_d - m)^2 - m^2 = -B_d M_d$$

$$\text{But } t^2 = (M_d + m)^2$$

$$\text{So } t^2 - M_t^2 = (M_d + m)^2 - M_t^2 = -2 M_t B_t$$

$$\text{where } B_d = 2M - M_d \text{ and } B_t = M_d + M - M_t$$

So we can see that contribution to scattering cross section from (fig. 7) is 80 times more than that from (fig. 8).

So for the time being we will forget about He^3 -pole term.

But, in the next chapter we will evaluate this pole contribution, because the presence of a $\text{He}^3\pi$ vertex makes the contribution comparably large.

3.4. The Vertex Functions And Form Factors:

The n-p-d vertex can be written as

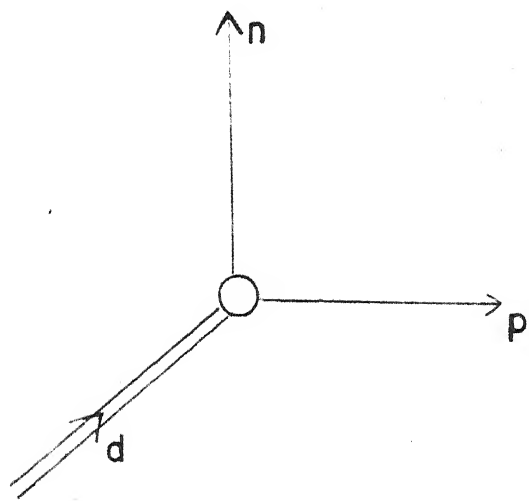
$$\bar{S}_{\alpha\beta} u_\alpha(p) u_\beta(n) \quad (18)$$

where $\bar{S}_{\alpha\beta}$ represent the creation of a deuteron in a triplet spin state. S can be written as

$$S = \int \zeta_\mu^\mu \quad (19)$$

where ζ_μ is polarisation 4-vector for spin one deuteron. First we will make a deuteron rest frame calculation and then generalise to arbitrary frame. To find out spin

Fig. 9



npd Vertex

structure of Γ^μ we note that it is proportional to a 4-vector λ^μ such that

$$\begin{aligned}\chi_{11} &= \vec{n} \uparrow \vec{p} \uparrow = \begin{bmatrix} 1 & 0 & 0 & 0 \\ 0 & 0 & 0 & 0 \\ 0 & 0 & 0 & 0 \\ 0 & 0 & 0 & 0 \end{bmatrix} = \frac{\lambda_x + i\lambda_y}{\sqrt{2}} \\ \chi_{10} &= \lambda_z, \chi_{1-1} = \frac{\lambda_x - i\lambda_y}{\sqrt{2}}\end{aligned}\quad (20)$$

one then obtains

$$= -\frac{i\lambda}{\sqrt{2}} \cdot (1 + \beta) \vec{\gamma}^0 \quad (21)$$

where $C = \gamma_0 \gamma_2$. The s and d-state wave function for deuteron are given by

$$\begin{aligned}\varphi_s &= \frac{u(r)}{r} Y_{101}^m \\ \varphi_d &= \frac{w(r)}{r} Y_{121}^m\end{aligned}\quad (22)$$

If p_s and p_d are corresponding probabilities we have $p_s + p_d = 1$. Similarly we write

$$\vec{\Gamma} = \vec{\Gamma}_s + \vec{\Gamma}_d \quad (23)$$

so that Y_{101}^m is proportional to χ_{11} and so on. Forming the correct vectors we find

$$\vec{\Gamma}_s \sim \sqrt{\frac{1}{4\pi}} \vec{\lambda} a_s, \vec{\Gamma}_d \sim \left(\sqrt{\frac{1}{8\pi}} \vec{\lambda} + \sqrt{\frac{1}{8\pi}} \frac{(k \cdot \vec{\lambda}) \vec{k}}{k^2} \right) a_d \quad (24)$$

where a_s and a_d are coefficients of leading terms of deuteron wave function in asymptotic expansion i.e.

$$\varphi(r) \sim e^{-\alpha r} [a_s + a_d x(\text{d state functions})] \quad (25)$$

Consequently

$$a_{s,d} = \text{Lt } (k^2 + \alpha^2) \varphi_{s,d}(k^2) \quad (25)$$

$\xrightarrow{-k^2 \rightarrow \alpha^2}$

where $\varphi_{s,d}(k^2)$ are the fourier transforms of deuteron s and d state wave functions.

Now the problem remains to generalise equation (21) into an arbitrary frame and then to make an off-shell correction. For the first case we just write

$$\lambda_\mu = \frac{i}{\sqrt{2}} \frac{(\gamma \cdot d + M_d)}{M_d} \gamma_\mu c \quad (26)$$

For the second problem we note that k is half of the relative momentum of proton and neutron when deuteron is at rest. If we define

$$k_\mu = (0, \vec{k})$$

and

$$d_\mu = (M_d, 0)$$

We have

$$k \cdot d = 0$$

As this is an invariant, $k \cdot d$ should also be zero in the moving frame.

Thus we get

$$k_\mu = -p_\mu + \frac{(p \cdot d)}{M_d^2} d_\mu \quad (27)$$

Consequently

$$\vec{k}^2 = [n^2 - (M_d + m)^2] [n^2 - (M_d - m)^2] / 4M_d^2$$

This suggests that the new value of k^2 not only takes care of moving deuteron, but also the situation when neutron is off the mass shell. Then we have the most plausible modification to make i.e. to remove the restriction of $-k^2 \rightarrow \alpha^2$ in equation (25) and write

$$a_{s,d} = \frac{k^2 + \alpha^2}{4\pi} \varphi_{s,d}(k^2) \quad (28)$$

Thus the vertex function can be written down as

$$\Gamma_\mu \sim (\gamma \cdot d + M_d) (k^2 + \alpha^2) \left[(\varphi_s(k^2) + \frac{\varphi_d(k^2)}{\sqrt{2}}) \gamma_\mu - \frac{3}{\sqrt{2}} \varphi_d(k^2) \frac{(\gamma \cdot k) k_\mu}{k^2} \right] c \quad (29)$$

Here we note that the contribution from d-state is only about 5 percent. So we can vary well write down

$$\varphi_d(k^2) = f \varphi_s(k^2) \quad (30)$$

To find out the multiplicative constant in (29) we assume that

$$M_d > M_p + M_n \quad (31)$$

Then deuteron will spontaneously decay into a proton and a neutron. The decay rate can be calculated from the figure 9 with the formula

$$\Gamma = \frac{k}{32\pi^2 M_d^2} \int \frac{4M_d^2 d\Omega}{(2s+1)} \quad (32)$$

where S is the spin of deuteron.

On the other hand equation (31) implies that asymptotic deuteron wave function should be

$$\varphi(r) \sim e^{-ikr} [a_s + a_d \text{ (d state functions)}]$$

As a result of this we have a decay rate for deuteron as

$$\Gamma = \frac{4\pi k}{E_p E_n} [|a_s|^2 + |a_d|^2] \quad (33)$$

Comparing equation (32) and (33) we obtain the constant in equation (29). Then neglecting d-state we have

$$\Gamma_\mu = \frac{4\pi N}{M_d^{3/2}} F_s(k^2) (\gamma_s d + M_d) \gamma_\mu c \quad (34)$$

with

$$F_s(k^2) = (k^2 + \alpha^2) \varphi_s(k^2)$$

$$\varphi_s(k^2) = \int d^3x e^{-ik_s x} \varphi_s(r) \quad (35)$$

$$= \frac{4\pi N(\beta^2 - \alpha^2)}{(\alpha^2 + k^2)(\beta^2 + k^2)} [\cos(kr_c) + \frac{\alpha\beta - k^2}{k(\alpha + \beta)} \sin(kr_c)] \quad (36)$$

$$\begin{aligned} \varphi_s(r) &= \frac{N}{r} [e^{-\alpha(r-r_c)} - e^{-\beta(r-r_c)}] \text{ for } r > r_c \\ &= 0 \text{ for } r < r_c \end{aligned} \quad (37)$$

$$N^2 = \frac{\alpha}{2\pi} \frac{\beta(\alpha + \beta)}{(\beta - \alpha)^2} = \frac{\alpha}{2\pi} \frac{e^{-2\alpha r_c}}{1 - \alpha \gamma_e} \quad (38)$$

γ_e is the effective range of deuteron. With this vertex, matrix element becomes

$$M = \frac{(4\pi N)^2}{M_d^3} \bar{u}(p')(\gamma \cdot d + M_d)(\gamma \cdot \xi) \cdot \frac{(\gamma \cdot n - m)}{n^2 - m^2} (\gamma \cdot \xi') (\gamma \cdot d' + M_d) \\ \times u(p) F^2(q^2) \quad (39)$$

with

$$\frac{d\sigma}{d\Omega} = \frac{1}{64\pi^2 W^2} \frac{1}{(2s_1+1)(2s_2+1)} |M|^2 \quad (40)$$

where s_1 and s_2 are spin of the initial particles.

3.5. Numerical Result And Discussion:

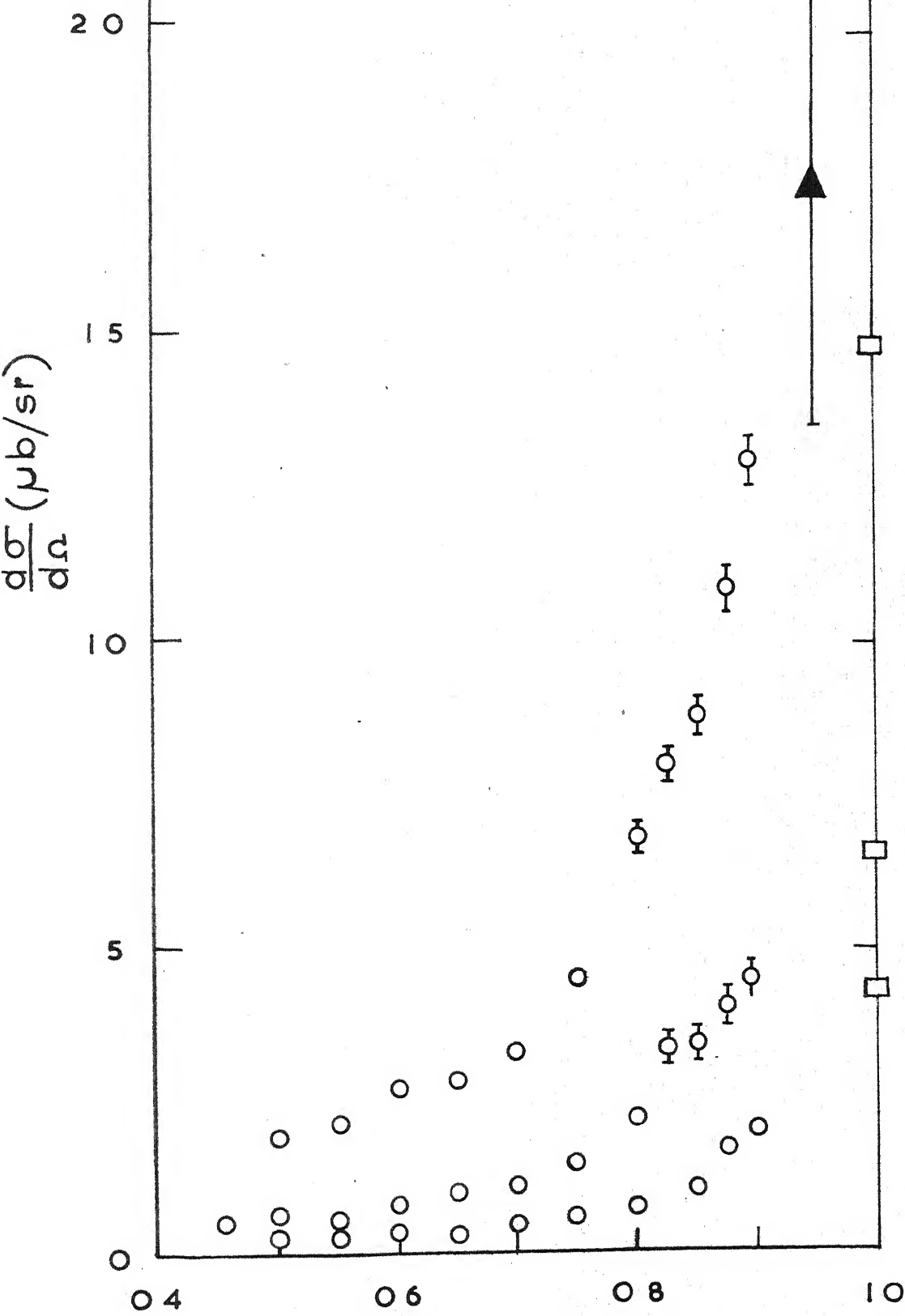
We have calculated the differential cross section at $(\cos\theta) = -1$ at energies 1.0, 1.3 and 1.5 Bev. There exists experimental data³⁹ for these energies, upto $\cos\theta = -1$. In figure 10 we have plotted our result at $\cos\theta = -1$ along with experimental points.

Our theory does not give good agreement for $\cos\theta > -1$. This may be due to the fact that vertex function and the form factor are not too good for high values of k^2 . It should be noted that we obtained equation (32) for $M_d > M_p + M_n$ and accepted in principle that the corresponding results will also be true when we extrapolate to the actual value of M_d . To keep the extrapolation meaningful the two values of M_d should be very nearly equal. This is true for the reason that α^2 is very small. At the same time we should also ensure that k^2 is very nearly zero. This criteria are satisfied only at $\cos\theta = -1$.

Another thing that we want to make clear is that the

Fig.10

BACKWORD PROTON-DEUTERON SCATTERING. THE CALCULATED VALUE AT 180° ARE SHOWN BY SQUARES



calculated cross section is very sensitive to the value of γ_e . We have used the value 1.43F, the value used by Gross⁵⁴. Bellac³¹ et al. have used the value around 1.6F. If one will analyse their results one will be convinced that they could have got the exact results with $\gamma_e \simeq 1.4F$. The experimental values are around 1.7F. But, these results are obtained from almost zero energy experiment. So a small energy dependent part in γ_e is not completely ruled out.

CHAPTER IV

PION PRODUCTION IN PROTON-DEUTERON COLLISION

In last Chapter we computed the proton deuteron elastic scattering with a nucleon pole diagram. In this Chapter we will deal with one proton deuteron **inelastic** collision. Explicitly, we will discuss the reaction,



This reaction was recently studied experimentally by Melissinos and Dahanayake³⁶ at proton kinetic energy $T_p = 1.515$ Bev at $\theta_{c.m.} = 0^\circ$. They obtain

$$\frac{d\sigma}{d\Omega} = (4.1 \pm 4) \times 10^{-32} \text{ cm}^2$$

Earlier Harting et al³⁷ observed the same reaction at $T_p = 600$ Mev and $\theta_{c.m.} = 52^\circ$. Their result is

$$\frac{d\sigma}{d\Omega} = (6.1 \pm 2) \times 10^{-30} \text{ cm}^2$$

It is observed that one result is hundred times larger than the other one. This is essentially attributed³⁶ to the rapid angular distribution which has been observed in other similar reactions.³⁹ To check this we have computed the differential cross section taking the Born diagrams. Our results also indicate rapid angular variation. Sometime back Mathews and Deo²⁶ Heintz et al²⁸ and Deo and Patnaik²⁷ computed the differential cross section for the reaction $p + p \rightarrow d + \pi^+$

with nucleon exchange and obtained many desirable results. We believe that the nucleon exchange also plays a dominant role in the reaction 1.

However there is another second order diagram (fig. 12) involving trition pole which is also important, particularly at lower energy. Here we report the results of our calculation with these two Feynman diagrams (fig. 11 and 12).

In Section 4.1 we indicate the outline of our calculation. In Section 4.2 the $pd\text{He}^3$ vertex is obtained. Section 4.3 deals with the discussion of $\text{He}^3\pi$ vertex and section V deals with numerical results and discussion.

4.1. Matrix Elements:

The invariant matrix element M can be written as

$$M = M_1 + M_2 \quad (2)$$

where M_1 and M_2 represent diagram 11 and 12 respectively.

The differential cross section is

$$\frac{d\sigma}{d\Omega} = \frac{1}{64\pi^2 W^2} \frac{p_f}{p_i} \frac{1}{(2s_1+1)(2s_2+1)} \sum |M|^2$$

where p_i and p_f are initial and final three-momenta in centre of mass frame. s_1 and s_2 are spins of the initial particles and W is the centre of mass energy. In calculation of the scattering amplitude first thing we have to do is to evaluate He^3dp vertex. This vertex is similar to ndt vertex which has been discussed by Blankenbecler et al.²³

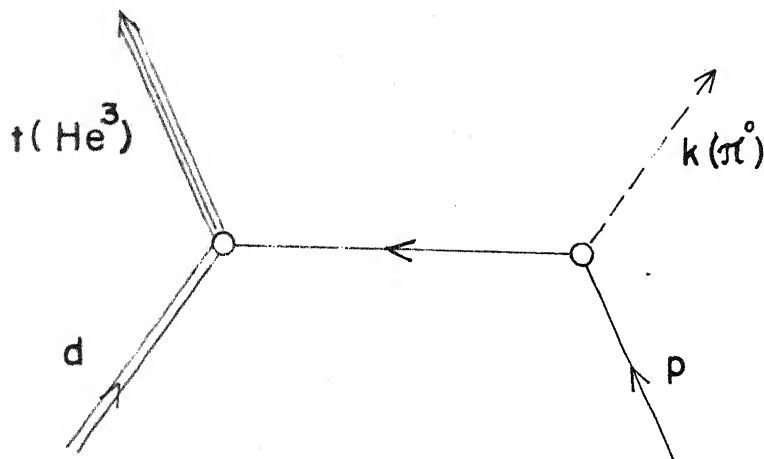


Fig.11

Feynman diagram for single-proton exchange in $p+d \rightarrow \text{He}^3 + \pi^0$

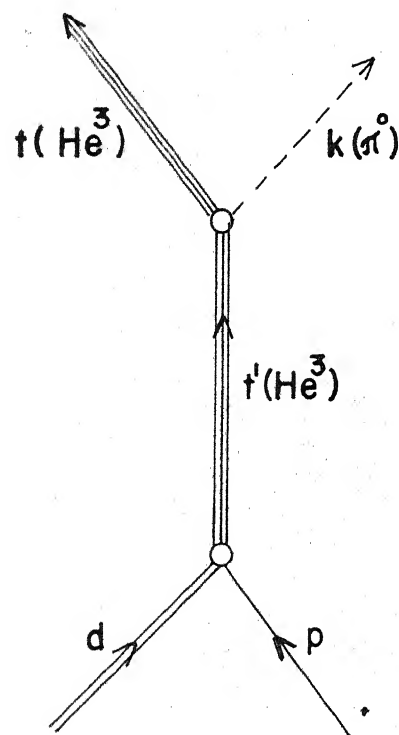


Fig.12

Feynman diagram for $p + d \rightarrow \text{He}^3 + \pi^0$ in direct channel with He^3 pole.

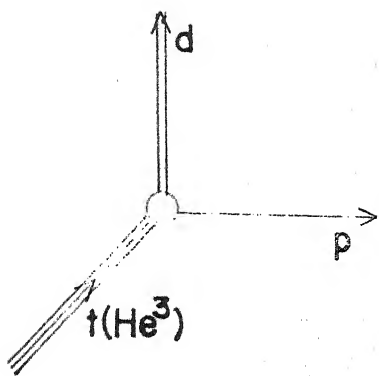


Fig. 13

$pdHe^3$ Vertex

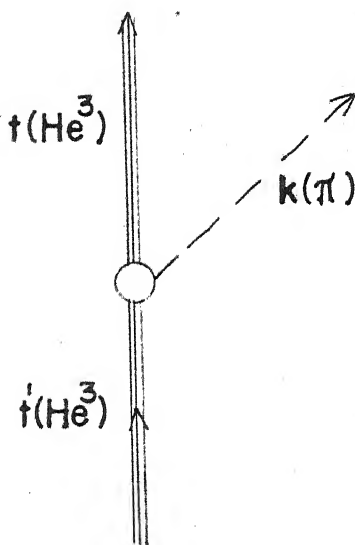


Fig. 14

$He^3He^3\pi^0$ Vertex

Their result for the vertex is given as (fig. 13)

$$\lambda \bar{u}(p) (\gamma \cdot \xi) \gamma_5 u(t) \quad (3)$$

where $u(p)$ and $u(t)$ are the spinors for proton and He^3 . We will use this vertex, but will calculate λ by Landau's⁴⁰ method with necessary modifications to include spin. Then we have

$$M_1 = g \bar{u}(t) (\gamma \cdot \xi) \gamma_5 (\gamma_p + m) \gamma_5 u(p) / (p^2 - m^2) \quad (4)$$

$$M_2 = G \bar{u}(t) \gamma_5 (\gamma \cdot t' + m) \gamma_5 (\gamma \cdot \xi) u(p) / (t'^2 - M_t^2) \quad (5)$$

where g is the pion nucleon coupling constant and $g^2/4\pi = 15$. G is the $\text{He}^3\pi$ coupling constant (fig. 14).

4.2. He^3 pd Vertex And Form Factors:

The He^3 pd vertex is $\lambda \bar{u}(p) (\gamma \cdot \xi) \gamma_5 u(t)$. To determine λ we calculate differential cross section for the process

$$p + d \rightarrow p + d \quad (6)$$

As the binding energy of He^3 is very small we write down the resonant scattering amplitude formula⁴¹

$$\frac{d\sigma}{d\Omega} = \frac{\hbar^2}{2\mu(E+B)} \quad (7)$$

for pd system. Here B is the binding energy of He^3 ($M_d + m - M_t$). M_t is the mass of He^3 , μ is reduced mass of pd system and

$$E = W - M_d - m$$

Now obtaining the contribution of fig. 16 and comparing with equation (7) at the pole, we obtain

$$\lambda^2 = 4\pi \frac{M_t}{m^2} [(m + M_d) B/3]^{\frac{1}{2}} \quad (8)$$

Next we calculate the form factor for the same vertex. This form factor is due to compositeness of the He^3 and is proportional to the Fourier transform of the He^3 wave function. The form factors go to one when the particles are put on the mass shell. Here we are concerned with He^3 going to $p + d$. So the wave function should be bound state wave function of p and d . So far this wave function has not been obtained. For simplicity we take a Hulthen type wave function.

$$\psi(r) = \frac{N}{r} [e^{-\alpha(r-r_c)} - e^{-\beta(r-r_c)}] \quad r > r_c \quad (9)$$

$$= 0 \quad r < r_c$$

where $\alpha = (2 \mu B)^{\frac{1}{2}}$ and r_c is the Hard core radius.

$$B = M_d + M - M_t$$

r_c = Hard core radius

This wave function for large distances behaves exactly as a bound state wave function of p and d .

To obtain N in 9, we imagine $M_t > M_d + m$, so that He^3 is unstable and decays into $p + d$. Matrix element describing this process is given by eqn.(3). If we represent the matrix element by T the decay rate is given by

$$T' = \frac{1}{32\pi^2 M_t^2} \frac{1}{2s+1} \int T^2 d\Omega \quad (10)$$

Now we consider He^3 mass moving into its correct value below $m + M_d$. Then the He^3 wave function changes from

$$N' e^{iqr/r} \quad (11)$$

to

$$N' e^{-\alpha r/r} \quad (12)$$

with

$$N' = \frac{e^{\alpha r}}{\sqrt{4\pi}} N \quad (13)$$

$$q^2 = [p^2 - (M_d + M_t)^2][p^2 - (M_t - M_d)^2]/4M_t^2$$

If we put the intermediate nucleon to the mass shell ($p^2 = m^2$) q^2 becomes $-\alpha^2$. Now equation 12 implies a decay rate.

$$T' = (4\pi q M_t / E_p E_d) N^2 \quad (14)$$

comparison of equations 10 and 14 gives

$$N^2 = \frac{\lambda^2 m}{3\pi} e^{-2\alpha r_c} \quad (15)$$

where we have put $M_t = 3m$, and $M_d = 2m$. On the other hand

we have

$$\int_{r_c}^{\infty} N^2 [e^{-\alpha(r-r_c)} - e^{-\beta(r-r_c)}]^2 dr = 1 \quad (16)$$

So we obtain a relation between β and r_c

$$N^2 = \frac{2\alpha\beta(\alpha+\beta)}{(\beta-\alpha)^2} = \frac{\lambda^2 m}{3\pi} e^{-2\alpha r_c} \quad (17)$$

Finally our form factor is given by

$$F(q^2) = (q^2 + \alpha^2) \varphi(q^2)$$

$$\varphi(q^2) = \frac{N(\beta^2 - \alpha^2)}{(q^2 + \alpha^2)(\beta^2 + q^2)} [\cos qr_c + \frac{\alpha\beta - q^2}{q(\alpha + \beta)} \sin qr_c]$$

(18)

and matrix elements

$$M_1 = \lambda g F(q^2) \bar{u}(t) (\gamma \cdot \xi) \gamma_5 \frac{(\gamma \cdot p' + m)}{p'^2 - m^2} \gamma_5 u(p) \quad (19)$$

$$M_2 = \lambda G F(q'^2) \bar{u}(t) \gamma_5 \frac{(\gamma \cdot t' + M_t)}{t'^2 - M_t^2} \gamma_5 (\gamma \cdot \xi) u(p) \quad (20)$$

$$q'^2 = [t'^2 - (M_d + m)^2][t'^2 - (M_d - m)^2] / 4M_t^2 \quad (21)$$

4.3. $\text{He}^3\text{He}^3\pi^0$ Coupling Constant:

To determine the value of G , we note that the triton and He^3 form an isospin doublet. By analogy with the pion-nucleon interaction we can write down a $\text{He}^3\pi$ interaction of the form

$$G \bar{\Psi}_H \gamma_5 \tau \cdot \varphi \Psi_H \quad (22)$$

The pion is coupled to He^3 through its coupling with the individual nucleons with the usual γ_5 interaction

$$g \bar{\Psi}_N \gamma_5 \tau \cdot \varphi \Psi_N \quad (23)$$

where

$$\Psi_H = \begin{pmatrix} \text{He}^3 \\ \text{H}^3 \end{pmatrix}, \Psi_N = \begin{pmatrix} p \\ n \end{pmatrix}$$

Our next job is to correlate G with g . To do this we assume that the fictitious processes $\text{He}^3 \rightarrow \text{He}^3 + \pi^0$ and $\text{He}^3 \rightarrow \text{He}^3 + \pi^+$ are allowed. We calculate the decay widths from (22) and (23) and compare. However, there are some difficulties. Inside He^3 there are two protons and one neutron. These two protons must obey the Pauli principle. When a neutron emits a π^0 , its spin may or may not flip. But the proton spin cannot flip when a π^0 is emitted. As a result, there will be a larger contribution to the non-spin-flip amplitude than to the spin-flip amplitude, and we shall not get the angular distribution expected from (22). So there must be some other constraints on the reaction so that we obtain the correct angular distribution. Here we discuss two possibilities of evaluating G without this difficulty.

(a) We assume that there exists some sort of correlation between the nucleons inside He^3 such that when one proton spin flips, the other proton also does. Then the Pauli principle is not violated and there will not be any restriction on spin-flip or non-spin-flip amplitudes. Then we obtain

$$G^2 = g^2 \quad (24)$$

(b) Recently Ericson and Locher⁴² have analysed πBe^9 system with forward dispersion relation and have obtained

$$f_{\text{eff}}^2 = .06$$

We know that for πN system

$$f^2 = .08 \text{ with } f^2 = \frac{g^2}{4\pi} \left(\frac{\mu}{2m}\right)^2$$

where μ and m are the pion and nucleon mass respectively.

As He^3 has all quantum numbers same as N and Be^9 except the baryon number and it comes in between N and Be^9 , we expect that the relation

$$f_{\text{N}}^2 \gg f_{\text{He}^3}^2 \gg f_{\text{Be}^9}^2$$

should be a valid one.

Now we have two values of G - one is g and the other one is slightly less than $3g$. In actual calculation we have taken G as a parameter and varied it in the range between g and $3g$. We found that the fit is better towards the higher limit of G .

4.4. Details of Trace Calculation:

We have the invariant matrix element

$$M = M_1 + M_2,$$

$$|M|^2 = |M_1|^2 + |M_2|^2 + (M_1^+ M_2 + M_2^+ M_1),$$

$$\sum |M_1|^2 = (A+B+C)F^2(q^2)/(p'^2-m^2)^2,$$

with

$$A = 12\lambda^2 g^2 [2(p.p' - m^2)(p'.t + mM_t) - (p.t + mM_t)(p'^2 - m^2)],$$

$$B = 4\lambda^2 g^2 (d.t/M_d^2) [2(d.p') (p.p' - m^2) - (p.d)(p'^2 - m^2)],$$

$$C = -4\lambda^2 g^2 [2(p'.t) (p.p' - m^2) - (p.t)(p'^2 - m^2)],$$

$$\sum |M_2|^2 = 4\lambda^2 G^2 [-3\mu^2 (p \cdot t + mM_t) + 4(k \cdot t)(-p \cdot k + \frac{(d \cdot p)(d \cdot k)}{M_d^2}) - 2\mu^2 (-p \cdot t + \frac{(d \cdot p)(d \cdot t)}{M_d^2}) + 6(k \cdot t)(p \cdot k)] XF(q^2)/(t^2 - M_t^2)^2,$$

$$\sum (M_1 M_2 + M_2 M_1) = 2\lambda^2 gGF(q^2)F(q^2)(X+Y+Z)/(p^2 - m^2)(t^2 - M_t^2),$$

with

$$X = -12[(p \cdot p' - m^2)(t \cdot t' - M_t^2) - (p \cdot t + mM_t)(p' \cdot t' + mM_t) + (p \cdot t + mM_t)(p \cdot t + mM_t)],$$

$$Y = -8[(t \cdot t' - M_t^2)(-p \cdot p' + \frac{(d \cdot p)(d \cdot p')}{M_d^2}) - (p \cdot t + mM_t)(-p \cdot p' + \frac{(d \cdot p)(d \cdot p')}{M_d^2})$$

$$+ (p \cdot t' + mM_t)(-p \cdot t + \frac{(d \cdot p')(d \cdot t)}{M_d^2})]$$

$$Z = 8[(t \cdot t' - M_t^2)(-p \cdot p' + \frac{(d \cdot p)(d \cdot p')}{M_d^2}) - (p \cdot t + mM_t)(-p \cdot p' + \frac{(d \cdot p)(d \cdot p')}{M_d^2})$$

$$+ (p \cdot t' + mM_t)(-p \cdot t + \frac{(d \cdot p)(d \cdot t)}{M_d^2})].$$

All these quantities were calculated by the usual techniques of trace and projection operators. For the deuteron polarizations we had

$$\sum |\xi|^2 = -3,$$

$$\sum (\xi \cdot A)(\xi \cdot B) = -(A \cdot B) + (d \cdot A)(d \cdot B)/M_d^2, d \cdot \xi = 0.$$

4.5. Numerical Results:

In this section we report the numerical calculations, using formulas of sections 4.1-4.4.

In figures 15-17 we draw the differential cross sections with .6 and 1.525 Bev proton laboratory kinetic energies. All the results are for the cut off $r_c = .052F$. The differential cross section for 0.6 Bev is plotted for two values of G (fig. 15). For 1.525 Bev the variation in backward differential cross section is negligibly very small. So we have plotted only one curve for $G = 2g$. In forward direction, however, the influence of G is quite significant. This we show in fig. 16 with three values of $G - 2g, 7g/3, 8g/3$. All these results are systematically put in the table I with experimental results.

The agreement with the experiment is quite good. Unfortunately there are no experimental results at backward angles to make any comparison. We have, however, calculated cross section at 180° with different energies (see table II). The cross section slightly increases with energy. We do not expect this increase. This is perhaps a bad feature of the model. Similar results were also obtained by others^{26,30} with nucleon exchange models.

Fig. 15

Differential Crosssection for the reaction $p + d \rightarrow \text{He}^3 + \pi^0$ at 0.6 Bev. with $r_c = 0.052$

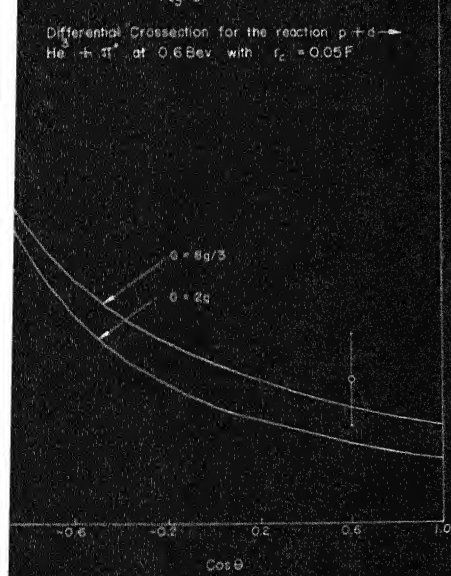


Fig. 16

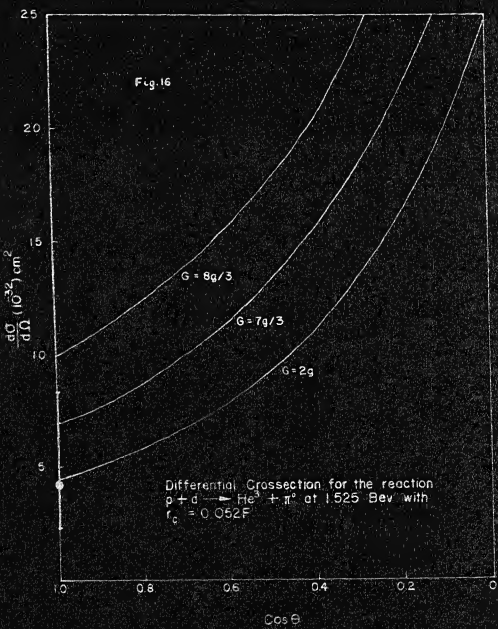


Fig. 17

Differential Crosssection for the reaction $p + d \rightarrow \text{He}^3 + \pi^0$ at 1.515 Bev. with $r_c = 0.052$ and $G \leq 2g$

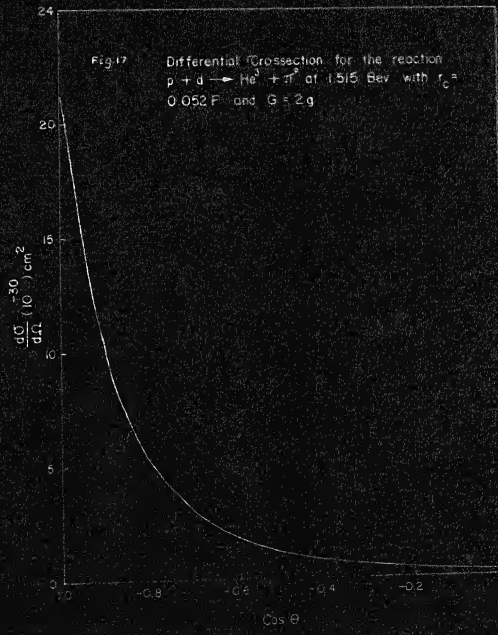


TABLE I
Differential Cross-section for $p+d \rightarrow \text{He}^3 + \pi^0$

G	r_c in Bev^{-1}	$\frac{d\sigma}{d\Omega} (10^{-32} \text{cm}^2)$ $T_p = 1.515 \text{Bev}$ $\Theta_{c.m.} = 0^\circ$	$\frac{d\sigma}{d\Omega} (10^{-30} \text{cm}^2)$ $T_p = .600 \text{Bev}$ $\Theta_{c.m.} = 52^\circ$
g	.168	7.0	2.1
	.220	2.29	1.88
2g	.220	12	3.8
	.270	4.5	3.4
	.319	1.96	3.0
7g/3	.220	18	4.6
	.270	6.9	4.2
	.319	2.36	3.77
8g/3	.220	24	5.59
	.270	9.94	5.0
	.319	3.08	4.50
Experiment		4^{+4}_{-2}	6 ± 2

Table II

Energy dependence of $\frac{d\sigma}{d\Omega}(10^{-30} \text{ cm}^2)$ at centre of mass angle
 180° for different values of r_c • $G = 2g$

T_p in Bev	r_c in Bev^{-1}	.22	.27	.31	.36	.41
1		19.8	19.5	19.2	18.9	18.6
2		22.6	22.3	22.1	21.8	21.6
3		24.2	24.0	23.8	23.5	23.5
4		25.4	25.1	24.9	24.7	24.4
5		26.2	25.9	25.7	25.4	25.1
6		26.8	25.5	26.2	25.9	25.5
7		27.2	26.9	26.6	26.2	25.7

CHAPTER VROLE OF NUCLEON EXCHANGE IN GENERATING He^3 POLE

In last two Chapters we have computed the differential cross sections of proton deuteron scattering, elastic as well as inelastic. In both the cases we have treated deuteron exactly in the same level as any other particles like proton or neutron. Our theories were developed on the framework of one particle exchange processes. In this Chapter we will present another working method in particle physics where one particle exchange is also important. We want to generate the He^3 -pole in pd scattering amplitude with nucleon exchange alone. As the mathematical tool we will use N/D method. The N/D method⁴³⁻⁴⁵ is a way to get the solution from dispersion relations. The equations are linear and they keep the scattering amplitude unitary. The input force is introduced through the N-function and the simultaneous equations are solved to obtain zeroes of D-function. The zeroes correspond to the bound states in that particular channel.

We will define proton-deuteron scattering amplitude in $J = \frac{1}{2}$, $l = 0$ channel as

$$M_{\frac{1}{2}} = \frac{E}{2iq} (e^{2i\delta} - 1) \quad (1)$$

$$\text{so that } \text{Im } M_{\frac{1}{2}} = \frac{p}{E} |M_{\frac{1}{2}}|^2 \quad (2)$$

subscript and write

$$\text{Im } M = \frac{p}{E} |M|^2$$

Then a dispersion relation for M can be written in the form

$$M(s) = A_0^B(s) + \frac{1}{\pi} \int_{-\infty}^{\infty} ds' \left(\frac{p'}{E'} \right) \frac{M(s')^2}{s' - s - i\epsilon} \quad (3)$$

$$(M_d + m)^2$$

$A_0^B(s)$ is the s -wave projection of Born amplitude. To get a solution to the equation we write

$$M = N/D \quad (4)$$

where N has all left hand singularities of M and D has all right hand singularities. With the help of unitarity relation the N/D equations become (Uretsky form)

$$N(s) = A_0^B(s) + \frac{1}{\pi} \int_{-\infty}^{\infty} ds' \left[A_0^B(s') - \frac{s - s_0}{s' - s_0} A_0^B(s) \right] \frac{N(s')}{s' - s} \frac{p'}{E'} \quad (5)$$

$$D(s) = 1 - \frac{s - s_0}{\pi} \int_{-\infty}^{\infty} ds' \left(\frac{p'}{E'} \right) \frac{N(s')}{(s - s)(s' - s_0)} \quad (6)$$

These two equations should be solved and zeroes of D should be obtained to give bound state and N/D at the pole to give coupling constant.

As the mass of He^3 is very close to the total mass of pd system the pole occurs very close to the threshold. This fact helps one to evaluate N/D even without knowing the input force. This is a very interesting situation and is

entirely due to the small binding energy of He^3 . From the equations 5 and 6 we write down

$$\frac{D}{N} \frac{(M_t^2)}{(M_t^2)} = \frac{1}{N(M_t^2)} \frac{1}{\pi} \int \frac{ds'}{(s' - M_t^2)} \frac{k'}{E'} N(s') \quad (7)$$

$$(M_d + m)^2$$

Now M_t being very close to $M_d + m$ the maximum contribution to the integral comes from the region close to the lower limit.

$\frac{N(s)}{E}$ is relatively slowly varying and can be taken out of the integral and given the value at the pole. Then we have

$$R^{-1} = \frac{1}{\pi M_t} \int \frac{ds}{(s - M_t^2)^2} \quad (8)$$

$$(M_d + m)^2$$

$$\text{where } k = [(s - (M_d + m)^2)(s - (M_d - m)^2)/4s]^{\frac{1}{2}} \quad (9)$$

The minimum value which s can take is $(M_d + m)^2$. So we can write

$$[s - (M_d - m)^2]^{\frac{1}{2}} = s^{\frac{1}{2}} \left[1 - \frac{(M_d - m)}{2s} \right] \quad (10)$$

Thus we obtain

$$R^{-1} = \frac{1}{\pi M_t} \int \frac{ds}{(s - M_t^2)^2} \left[\left(\frac{s - (M_d + m)^2}{4} \right)^{\frac{1}{2}} \cdot \left(1 - \frac{(M_d - m)^2}{2s} \right) \right] \quad (11)$$

Finally we obtain

$$R^{-1} = \frac{1}{\pi M_t} \left[1 - \frac{(M_d - m)^2}{2(M_d + m)^2} \right] \int_{(M_d + m)^2} \frac{ds}{s} \left[(s - (M_d + m)^2)/4 \right]^{1/2} / \left[s - (M_d + m)^2 + 2(M_d + m)B \right] \quad (12)$$

$$\text{Now put } x = [s - (M_d + m)^2] / [2(M_d + m)B]$$

$$\begin{aligned} \text{Then } R^{-1} &= \frac{1}{\pi M_t} \left(1 - (M_d + m)^2 / 2(M_d - m)^2 \right) [8(M_d + m)B]^{-1/2} \int \frac{dx}{(x+1)^2} x^{1/2} \\ &= (4M_t (2M_t B)^{1/2})^{-1} \left[1 - \frac{1}{2} (M_d - m)^2 / (M_d + m)^2 \right] \quad (13) \end{aligned}$$

and

$$R = \left[1 - \frac{1}{2} (M_d - m)^2 / (M_d + m)^2 \right]^{-1} \times 4 M_t (2M_t B)^{1/2} \quad (14)$$

Thus we have obtained the residue of the scattering amplitude at the pole. But, this does not give any ideas about the input force except that this gives the correct pole position. To see the nature of force between p and d we do the N/D calculation numerically with nucleon exchange as the input force. From equation 39 of Chapter III we write down the scattering amplitude.

$$M = \frac{(4\pi N)^2}{M_d^3} \bar{u}(p) (\gamma \cdot d + M_d) (\gamma \cdot \xi) \frac{(\gamma \cdot n - m)(\gamma \cdot \xi)}{(n^2 - m^2)} (\gamma \cdot d + M_d) u(p) \quad (15)$$

As we know that the maximum contribution to the scattering amplitude comes from the neighbourhood of threshold we make a non-relativistic approximation. This was the reason why we put the mass-shell value of the form factor in eqn.15.

Then we have

$$M = \frac{(4\pi N)^2}{M_d^3} 3mM_d^2 u^+(p') (\sigma \cdot \vec{\epsilon}) (\sigma \cdot \vec{\epsilon})^* u(p) / (n^2 - m^2) \quad (16)$$

We are interested in $\ell = 0, J = \frac{1}{2}$ state. To do this we first make the helicity decomposition⁴⁶ and then express the $\ell = 0, J = \frac{1}{2}$ amplitude in terms of the helicity amplitudes. For pd system there are 6 helicity states,

$$|1\frac{1}{2}\rangle, |1-\frac{1}{2}\rangle, |0\frac{1}{2}\rangle, |0-\frac{1}{2}\rangle, |1-1\frac{1}{2}\rangle, |1-1-\frac{1}{2}\rangle$$

There are, in total, 12 independent helicity amplitudes.

We have

$$\begin{aligned} | \ell = 0, J = \frac{1}{2} \rangle &= \frac{1}{\sqrt{3}} (|1\frac{1}{2}\rangle - |1-1\frac{1}{2}\rangle \\ &+ \frac{1}{\sqrt{6}} (|0\frac{1}{2}\rangle - |0-\frac{1}{2}\rangle) \end{aligned} \quad (17)$$

Consequently the $\ell = 0, J = \frac{1}{2}$ amplitude is

$$\begin{aligned} M &= \frac{1}{3} [2 (\langle 1\frac{1}{2} | M | 1\frac{1}{2} \rangle - \langle 1\frac{1}{2} | M | -1-\frac{1}{2} \rangle) \\ &+ \langle 0\frac{1}{2} | M | 0\frac{1}{2} \rangle - \langle 0\frac{1}{2} | M | 0-\frac{1}{2} \rangle \\ &+ \sqrt{2} (\langle 1\frac{1}{2} | M | 0\frac{1}{2} \rangle - \langle 0\frac{1}{2} | M | 0-\frac{1}{2} \rangle)] \end{aligned} \quad (18)$$

Finally for Born amplitude we obtain

$$\begin{aligned} A_0^B(s) &= \left(\frac{8\alpha}{1-\alpha\gamma_e} \right) \frac{E_p + m}{2m} (1/6q^2) [C (-2A + A^2 \log \frac{A+1}{A-1}) \\ &+ D \log \frac{A+1}{A-1}] \end{aligned}$$

where

$$\begin{aligned}
 A &= (C^2 - M_d^2)/2q^2 \\
 C &= 1 - E_d/M_d + (E_d/M_d)^2 \\
 D &= 1 + E_d^2/2M_d^2
 \end{aligned} \tag{19}$$

With $A_c^B(s)$ as the input force we solved the N/D equations. We obtained a bound state with all the quantum numbers of He^3 . However the mass of the predicted particle is more than the mass of He^3 . The mass of He^3 is 2.808 Bev whereas we obtained 2.813 Bev. This discrepancy may be due to the presence of the 3-particle inelastic ^{cut} which starts very close to the elastic cut. At 1 Bev the ratio of total scattering cross section to elastic scattering cross section ^{47,48} is slightly more than 6. Most of the inelastic contribution comes from the deuteron disintegration. There is no method to include 3-body reaction within the N/D approach. The best one can do is to introduce a parameter $R(s)$ ⁴⁴⁻⁴⁵ in eqn. 2.

$$\text{Im } M = R(s) \frac{p}{E} |M|^2 \tag{2a}$$

Below the inelastic threshold $R(s) = 1$. In general it is

$$R_1(s) = \frac{\sigma(\text{total})}{\sigma(\text{elastic})} \tag{20}$$

We repeated the calculation with different values of $R(s)$ and found that the result significantly improves with higher values of $R(s)$. More ever we have completely ignored the contributions from the t-channel exchanges.

To summarise, we note that there is a pole in p-d amplitude corresponding to the quantum numbers of He^3 . The pole position does not coincide with that of He^3 , but the pole position changes if we change the strength of interaction between p and d. Then, according to Weinberg's criteria², deuteron is a composite particle. In the same yardstick nucleon is also a composite state of $\text{N}^*\pi$. This suggests the equal status for all particles..

CHAPTER VI

ON THE EXISTENCE OF PEAKS IN THE CROSS SECTION OF THE REACTIONS, $p+p \rightarrow d+\pi^+$, $k+d \rightarrow p+\Delta$, $p+d \rightarrow \text{He}^3+X$

The peaks in the pion nucleon and kaon nucleon scattering cross sections are explained through the existence of a large number of $N\pi$ and NK resonances. These resonances do really exist and can also be produced in the laboratory. In contrast, there exist a few reactions where the peaks in the cross section can not be explained like this. For example, consider the reactions



and



A few peaks have been observed in the reactions 1 and 2. In the reaction 1 a peak is found at 2.2 Bev centre of mass energy and another at about 3.0 Bev. This should suggest that there exists two pp resonances with masses 2.2 and 3 Bev. As a result, we should also be able to observe peaks in the pp elastic cross section. No such peaks have been observed. [There has been, however, a considerable ⁴⁹ speculations about the existence of $B=2$ resonances.] In what follows, we will point out that the peaks are entirely due to the small binding energy of the deuteron and we will calculate analytically the positions of the peaks for the

reactions 1 and 2 and for the reaction



where X is a neutral meson. This experiment is presently being conducted at several centres. So the results can be verified very soon.

The diagram which is responsible for the peaks in the reaction 1 is shown in fig. 18. Following Yao²⁹ we write

$$d^4 n_1 = \int d n_1^2 d p_1^2 d k_1^2 ds \quad (4)$$

and put effectively n_1 and p_1 on the mass shell through contour integrations. When deuteron is at rest we have

$$E_{p_1} = \frac{M_d}{2}, \quad p_1^2 = -\alpha^2 \quad (5)$$

with $\alpha^2 = m B$, where m is the mass of the nucleon and B is the binding energy of the deuteron. Now we expect a peak in the cross section when

$$(p_1 + k)^2 - M^*^2 = 0 \quad (6)$$

where M^* is the mass of a pion nucleon resonance. In the deuteron rest frame

$$(p_1 + k)^2 = m^2 + \mu^2 + 2 \left[\frac{M_d}{2} E_k - i \alpha \vec{k} \cdot \vec{p}_1 \cos \beta \right] \quad (7)$$

As α is very small compared to M_d we may neglect the last term and get

$$(p_1 + k)^2 = m^2 + \mu^2 + M_d E_k \quad (8)$$

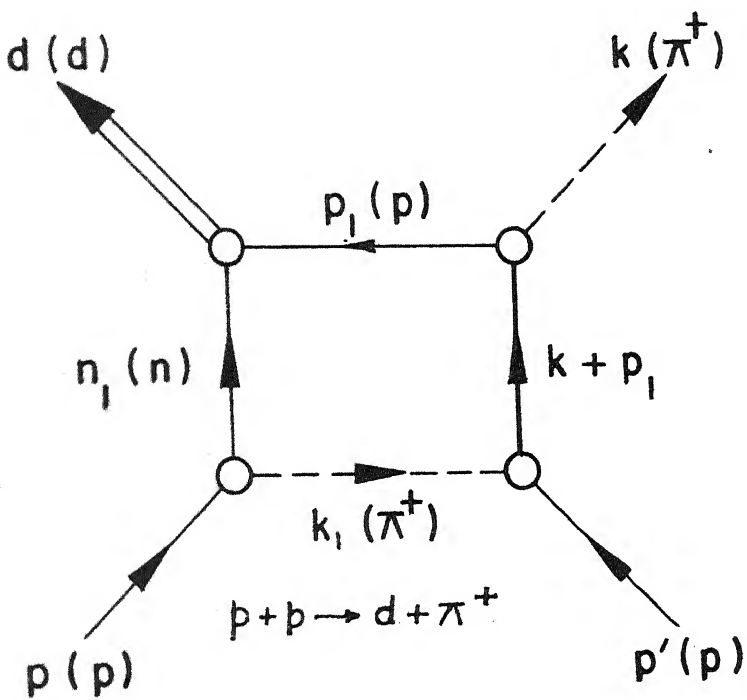


Fig. 18

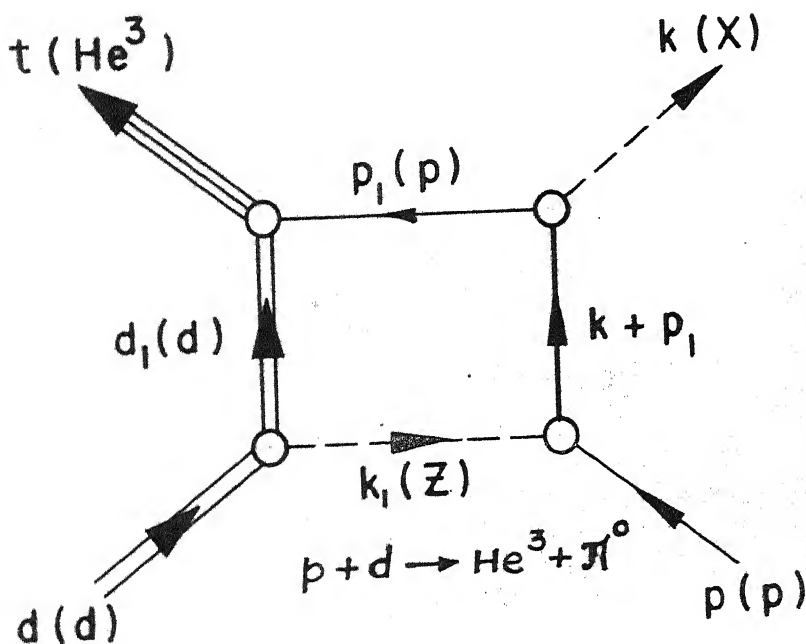


Fig. 19

Also in the deuteron rest frame the Mandelstam variable s can be written as

$$s = (d+k)^2 = M_d^2 + \mu^2 + 2E_k M_d \quad (9)$$

From equations 8 and 9 the positions of the peaks are given by

$$W^2 = s = 2(m^2 + M^2) - \mu^2 \quad (10)$$

where W is the centre of mass energy.

The resonance state is predominantly a $I = 3/2$ state. $I = \frac{1}{2}$ state contribution is supposed to be small. The formula (10) fits quite nicely with the observed peaks.⁵⁰ D.J. Brown⁵¹ has mentioned about the experiment done by Hinks, where he has observed some more peaks. These are also consistent with our formula.

The same formula also holds good for the reaction 2 where μ is the mass of the K meson and M is the mass of a $K-N$ resonance ($I = \frac{1}{2}$).

Now we apply the same technique for the reaction 3. The corresponding diagram is given in fig. 19. The essential difference of this process from the reaction 1 is that Z is a $I = 0$ boson or a photon. When Z is a isosinglet boson the resonance state is a $I = \frac{1}{2}$ state. For the photon exchange there can be a $I = 3/2$ state also. But, this will be very small. We supply adequate form factors (form reaction 1 it is

Ferrari-Selleri form factors) to make the integral convergent we follow all the prescriptions as in the case of reaction 1. Then the peaks for this reaction will be given by

$$w^2 = 6m^2 + 3M^2 - 2\mu^2 \quad (11)$$

In table 3 bellow we give the positions of the peaks for the different final state particles.

We believe that the contributions from diagram 1 and 2 along with the nucleon exchange diagrams should be good approximations for the corresponding reactions.

Although the nucleon exchange mechanism^{26-28,52} have been able to explain many features, it has failed completely to explain energy dependence.^{26,51} Better nucleon exchange models have to be tried before a unified version is attempted.

Finally, we must point out that the existence of the peaks in these reactions can also be inferred from the absorption models²¹ and with the help of impulse approximation.⁵ In the absorption model the Born matrix elements are modified with the corresponding initial and final state matrix elements. In reaction 1, for example, we will have a multiplicative factor with the matrix element for $\pi^+ + d \rightarrow \pi^+ + d$. Through impulse approximation, this can be related to $\pi^+ N$ scattering cross section which contains many peaks. As a result, we will have peaks in the cross section of reaction 1.

TABLE III
Position of peaks for different final state particles

X	Position of the peak (M)	Contributing resonance
$\pi^0(135)$	3.438 3.487 3.714 4.431 5.130	N^* $\frac{1}{2}$ (1470) N^* $\frac{1}{2}$ (1525) N^* $\frac{1}{2}$ (1688) N^* $\frac{1}{2}$ (2200) N^* $\frac{1}{2}$ (2650)
$\gamma(549)$	3.355 3.406 3.638 4.367 5.075	N^* $\frac{1}{2}$ (1470) N^* $\frac{1}{2}$ (1525) N^* $\frac{1}{2}$ (1688) N^* $\frac{1}{2}$ (2200) N^* $\frac{1}{2}$ (2650)
$\omega(783)$	4.296 5.013	N^* $\frac{1}{2}$ (2200) N^* $\frac{1}{2}$ (2650)
$\rho(770)$	4.30 5.017	N^* $\frac{1}{2}$ (2200) N^* $\frac{1}{2}$ (2650)
$A_1(1070)$	4.169 4.905	N^* $\frac{1}{2}$ (2200) N^* $\frac{1}{2}$ (2650)

CHAPTER VII

CONCLUSION

In this thesis we have considered several reactions which involve deuterons and He^3 . The prime motivation was to treat deuteron and He^3 as single particles rather than systems of particles. These reactions have been described separately where we have also mentioned the successes and failures of this approach. To conclude, however, we make a few general observations.

The theoretical results we have obtained are in fair agreement with the available experimental findings. The backward cross section for the reaction $p+d \rightarrow \text{He}^3 + \pi^0$ shows slight increase with energy. Although no experimental data are available for this region we do not anticipate this increase. Similar results were also reported previously for the reaction $p+p \rightarrow d + \pi^+$. However, the (backward) energy dependence is quite good for elastic cross section. The results of Chapter VI are most interesting. We predict the positions of the peaks for the reactions, $p+p \rightarrow d + \pi^+$, $d+k \rightarrow p+\Lambda$ and $p+d \rightarrow \text{He}^3 + X$ without assuming the existence of two or three baryon resonances. The experimental results are available for the reaction $p+p \rightarrow d + \pi^+$ and these are consistent with our results.

Thus we have been partly successful in describing composite particles like deuteron and He^3 as single particles

like p and Λ . There have been arguments in favour of giving equal status for all particles.¹ The approach we have pursued may not be in itself enough to prove it, but the results we have obtained are sufficient to keep our interests alive and undertake further investigations.

APPENDIX

MORE ABOUT npd VERTEX

In this appendix we will first discuss the npd vertex derived by Mathews and Deo.²⁶ We will utilise their result to obtain a more general vertex which goes to Blankenbecler, Goldberger, Halpern²³ vertex in the neighbourhood of the pole. When the intermediate particle is exactly on the mass shell this result coincides with the result of Deo, Mathews and Blankenbecler, Goldberger, Halpern. At the end we show the explicit relation between the form factor and the deuteron wavefunction.

Al. Mathews-Deo Vertex²⁶

Mathews and Deo write down the dnp vertex as

$$\bar{u}(n) [g_1(\gamma \cdot \xi) + g_2(p \cdot \xi)] v(p) \quad (Al)$$

where u and v are particle and antiparticle spinors respectively, g_1 and g_2 are real constants and are determined in the following manner.

Assuming that $M_d > m_p + m_n$ the matrix elements can be calculated for the process $d \rightarrow n+p$ in different spin states. This can be done in two ways - directly from vertex Al and by Clebsch-Gordan coefficients in terms of two amplitudes f_s and f_d . These f_s and f_d can, in turn, be related to parameters of asymptotic non-relativistic

Schroedinger wavefunction. By equating the results from these two methods they obtained

$$\begin{aligned}
 g_1 &= 4\pi \left[\frac{F_p F_n M_d^3}{E_p E_n} \right]^{\frac{1}{2}} \frac{1}{F_p F_n + q^2} \left(a_s + \frac{a_d}{\sqrt{2}} \right) \\
 g_2 &= 8\pi \left[\frac{F_p F_n M_d^3}{E_p E_n} \right]^{\frac{1}{2}} \frac{1}{(F_p F_n + q^2)(F_p + F_n)} \\
 &\quad \times \left(a_s - \frac{a_d}{\sqrt{8}} \frac{3F_p F_n + q^2}{q^2} \right) \tag{A2}
 \end{aligned}$$

where

$$\begin{aligned}
 E_p &= (M_d^2 - m_p^2 - m_n^2)/2M_d \\
 E_n &= (M_d^2 - m_n^2 - m_p^2)/2M_d \\
 F_p &= [(M_d + m_p)^2 - m_n^2]/2M_d \\
 F_n &= [(M_d + m_n)^2 - m_p^2]/2M_d \\
 q^2 &= [n^2 - (M_d + m_p)^2] [n^2 - (M_d - m_n)^2]/4M_d^2 \tag{A3}
 \end{aligned}$$

a_s and a_d are defined in Chapter III, equation 25.

A2. Generalised Vertex

Instead of equation A1 we can also write

$$\bar{u}(n) (\gamma \cdot d + M_d) [G_1(\gamma \cdot \xi) + G_2(\gamma \cdot k) (k \cdot \xi)] v(p) \tag{A4}$$

with

$$k_\mu = -n_\mu + \frac{(d \cdot n)}{M_d^2} d_\mu \tag{A5}$$

On the mass shell (A4) reduces to (A1)

with

$$\begin{aligned} g_1 &= 2 G_1 M_d \\ g_2 &= 2 G_1 - G_2 M_d \end{aligned} \quad (A6)$$

or

$$\begin{aligned} G_1 &= \frac{A}{2M_d} \left(a_s + \frac{a_d}{\sqrt{2}} \right) \\ G_2 &= \frac{A}{2M_d^3} \frac{a_d}{\sqrt{2}} \frac{3(F_p F_n + q^2)}{q^2} \\ A &= 4\pi \left(\frac{F_p F_n M_d^3}{E_p E_n} \right)^{\frac{1}{2}} \frac{1}{F_p F_n + q^2} \end{aligned} \quad (A7)$$

Then the vertex function becomes (apart from a multiplicative constant)

$$\frac{A}{2M_d} \bar{u}(n) (\gamma \cdot d + M_d) \left[\left(a_s + \frac{a_d}{\sqrt{2}} \right) (\gamma \cdot \xi) + \frac{3a_d}{\sqrt{2}M_d^2} \frac{M_d^2 + q^2}{q^2} \right. \\ \left. (\gamma \cdot k) (k \cdot \xi) \right] v(p) \quad (A8)$$

where

$$k^2 = -q^2$$

Here we wish to point out that the pole at $q^2 = 0$ is not to be found any more.

A3. Blankenbecker, Goldberger and Halpern Vertex²³

Close to the pole we have

$$a_s \approx 1$$

$$a_d \approx \rho$$

$$q^2 \approx 0$$

$$\bar{u}(n) (\gamma \cdot d + M_d) \left[\left(1 + \frac{\rho}{\sqrt{2}} \right) (\gamma \cdot \xi) - \frac{3}{\sqrt{2}} \frac{(\gamma \cdot k)(k \cdot \xi)}{k^2} \right] v(p) \quad (A9)$$

A4. Form Factor And Deuteron Wavefunction

We can separate the spin part of the vertex and write $\Gamma = HS$. H can be written as⁵³

$$H = \langle \varphi(r) | v(r) | e^{-iq \cdot r} \rangle \quad (A10)$$

The Schroedinger equation now reads as

$$\left[- \frac{\nabla^2}{m} + V(r) \right] \varphi(r) = - B \varphi(r) \quad (A11)$$

So that

$$\begin{aligned} H &= - \frac{1}{m} \langle \varphi(r) | Bm - \nabla^2 | e^{-iq \cdot r} \rangle \\ &= - \frac{1}{m} (\alpha^2 + q^2) \langle \varphi(r) | e^{-iq \cdot r} \rangle \end{aligned}$$

which is equal to

$(\alpha^2 + q^2) \varphi(q^2)$ apart from a multiplicative constant. $\varphi(q^2)$ is the Fourier transform of the deuteron wave function.

Thus we have correlated the form factor with deuteron wave function.

REFERENCES

1. G.F. Chew in Strong Interaction Physics, Benjamin, New York, 1964
2. S. Weinberg, Phys. Rev. 130, 776 (1963)
3. M.L. Goldberger and K.M. Watson, Collision Theory, John Wiley, New York, 1964
4. R.G. Newton, Scattering Theory of Waves and Particles, McGraw-Hill, New York, 1966
5. R.J. Glauber, Phys. Rev. 100, 242 (1955)
R.J. Glauber in Lectures in Theoretical Physics, edited by W. Brittin et al., Inter Science, New York, 1959
6. B.M. Udgaonkar and M. Gell-Mann, Phys. Rev. Letters 346 (1962)
7. E.S. Abers, H. Burkhardt, V.L. Teplitz, C. Wilkin, Cern Preprint, 65/1341/5-TH 602
8. A.N. Mitra, Phys. Rev. 123, 1892 (1961), 127, 1342 (1962) and Nucl. Phys. 32, 529 (1962)
9. T. Mongan, Phys. Rev. 147, 1117 (1966)
10. R. Aaron, R.D. Amado, Y. Yam Phys. Rev. 140, B1291 (1965)
11. There are excellent text books and monographs on field theory. In the present work we will follow the notations and conventions of
S.S. Schweber, In Introduction to Quantum Field Theory, Harper and Row, New York, 1961
12. H.A. Bethe and F. de Hoffman, Mesons and Fields, Vol. II, Mesons, Row, Peterson and Co., Evanston, Illinois
13. See ref. 11
14. G.F. Chew, S-Matrix Theory of Strong Interactions, Benjamin, New York, 1961
15. S. Mandelstam, Phys. Rev. 112, 1344 (1958) and Phys. Rev. 115, 1741, 1752 (1959)

16. A.C. Hearn and S.D. Drell, Peripheral Process, in High Energy Physics, Vol. II, edited by E.H.S. Burhop, Academic Press, New York, 1967
17. E. Ferrari and F. Selleri, Nuovo Cim. Suppl. 24, 453 (1962)
- 17a. F. Selleri, Lectures in Theoretical Physics, Vol. VIIb, University of Colorado Press (1964)
18. E.J. Squires, Complex Angular Momenta and Particle Physics, Benjamin, New York, 1963
19. B.M. Udgaonkar, Phenomenology based on Regge Poles, in Strong Interaction and High Energy Physics, edited by R.G. Moorhouse, Oliver and Boyd. 1964
20. F. Zachariasen, The Theory and Applications of Regge Poles, in 1962 Cargese Lectures in Theoretical Physics, Benjamin, New York, 1963
21. For a simple but elegant discussion, see S. Gasiorowicz, Elementary Particle Physics, Wiley and Sons, 1967. References to original papers can be found there.
22. M. Baker and R. Blankenbecler, Phys. Rev. 128, 415 (1962)
23. R. Blankenbecler, M.L. Goldberger and F.R. Halpern, Nucl. Phys. 12, 629 (1959)
24. J. Bernstein, Phys. Rev. 129, 2323 (1963)
25. J. Nearing, Phys. Rev. 132, 2323 (1964), 135, AB2 (1964)
26. J. Mathews and B. Deo, Phys. Rev. 143, 1340 (1966)
27. B. Deo and P.K. Patnaik, Proceedings of 9th Symposium on Cosmic Rays, Elementary Particles and Astrophysics, Bombay, 1965 (Unpublished)
28. R.M. Heinz, O.E. Overseth, M.H. Ross, Bull. Am. Phys. Soc. 10, 19 (1965). See also R.M. Heinz, Doctoral thesis, University of Michigan, 1964 (Unpublished).
29. T. Yao, Phys. Rev. 134, B454 (1964)
30. D.J. Brown, Nucl. Phys. B7, 37 (1968)
31. M. Gourdin, J. Le Bellac, F.M. Renard, 27 524 (1965)

32. A.K. Kerman and L.S. Kisslinger, High Energy Proton-Deuteron Scattering and Baryon Resonances in Nuclear Matter, M.I.T. Preprint (1968)

33. L.D. Fadeev, Zh. Eksperim i Teor.-Fiz. 39, 1459 (1960), English translation: Soviet Phys.- J.E.T.P. 12, 1014 (1960)

34. J. Gillepsie, Phys. Rev. 160, 1432 (1968)

35. V.A. Alessandrini, H. Fanchiotti and C. Garcia, Trieste Preprint IC/68/5

36. A.C. Melissions and C. Dahanayake, Phys. Rev. 159, 1210 (1967)

37. D. Harting et al., Phys. Rev. Letters 3, 52 (1959)

38. E. Coleman et al., Phys. Rev. Letters 16, 761 (1966)

39. O.E. Overseth et al., Phys. Rev. Letters 13, 59 (1964)

40. L.D. Landau, Zh. Eksperim. i Teor. Fiz 39, 1856 (1960), English translation: Soviet Physics-J.E.T.P. 12, 1294 (1961). See also M. Nauenberg, Phys. Rev. 124, 2011 (1961), G. Barton, Dispersion Techniques in Field Theory, Benjamin, New York, 1965 (p.196)

41. L.D. Landau and E.M. Lifshitz, Quantum Mechanics, Addison-Wesley, Reading, Mass, 1958

42. T.E.O. Ericson and M.P. Locher, Phys. Letters 26B, 91 (1968)

43. B.M. Udgaonkar, in High Energy Physics and Elementary Particles (P.791) I.A.E.A. Vienna (1965)

44. E. Abers and C. Zemach, Phys. Rev. 131, 2305 (1963)

45. L.A.P. Balazs, Lectures on Bootstrap Dynamics, Delhi University Summer School, 1965 (Unpublished)

46. M. Jacob and G.C. Wick, Ann. Phys. 7, 404 (1959)

47. G.W. Bennet, et al., Phys. Rev. Letters 19, 387 (1967)

48. D.V. Bugg et al., Phys. Rev. 146, 980 (1966)

49. F.J. Dyson and N.H. Xuong, Phys. Rev. Letters 13, 815 (1964) and 14, 339 (1965)

J. Kidd et al., Phys. Letters 16, 75 (1965)

50. See ref. 29 for experimental results
51. D.J. Brown, Nucl. Phys. B7, 37 (1968)
52. P.K. Patnaik, Phys. Rev. 175, 2069 (1968)
53. G.F. Chew and M.L. Goldberger, Phys. Rev. 77, 470(1964)
54. F. Gross, Phys. Rev. 136, B140 (1964).